Zoological Journal of the Linnean Society, 2022, **XX**, 1–20. With 9 figures.

Cranial osteology and palaeobiology of the Early Cretaceous bird *Jeholornis prima* (Aves: Jeholornithiformes)

HAN HU[1,*], YAN WANG[2,*], MATTEO FABBRI[3], JINGMAI K. O'CONNOR[3,4,5], PAUL G. MCDONALD[6], STEPHEN WROE[6], XUWEI YIN[7], XIAOTING ZHENG[2,7], ZHONGHE ZHOU[4,5] and ROGER B. J. BENSON[1]

[1]*Department of Earth Sciences, University of Oxford, Oxford OX1 3AN, UK*
[2]*Institute of Geology and Paleontology, Linyi University, Linyi, Shandong 276000, China*
[3]*Negaunee Integrative Research Center, Field Museum of Natural History, Chicago, IL 60605, USA*
[4]*Key Laboratory of Vertebrate Evolution and Human Origins, Institute of Vertebrate Paleontology and Paleoanthropology, Chinese Academy of Sciences, 100044 Beijing, China*
[5]*Center for Excellence in Life and Paleoenvironment, Chinese Academy of Sciences, 100044 Beijing, China*
[6]*Zoology Division, School of Environmental and Rural Sciences, University of New England, Armidale, NSW 2351, Australia*
[7]*Shandong Tianyu Museum of Nature, Pingyi, Shandong, China*

Received 11 July 2022; revised 2 September 2022; accepted for publication 7 September 2022

Jeholornis is a representative of the earliest-diverging bird lineages, providing important evidence of anatomical transitions involved in bird origins. Although ~100 specimens have been reported, its cranial morphology remains poorly documented owing to poor two-dimensional preservation, limiting our understanding of the morphology and ecology of the key avian lineage Jeholornithiformes, in addition to cranial evolution during the origin and early evolution of birds. Here, we provide a detailed description of the cranial osteology of *Jeholornis prima*, based primarily on high-quality, three-dimensional data of a recently reported specimen. New anatomical information confirms the overall plesiomorphic morphology of the skull, with the exception of the more specialized rostrum. Data from a large sample size of specimens reveal the dental formula of *J. prima* to be 0–2–3 (premaxillary–maxillary–dentary tooth counts), contrary to previous suggestions that the presence of maxillary teeth is diagnostic of a separate species, *Jeholornis palmapenis*. We also present evidence of sensory adaptation, including relatively large olfactory bulbs in comparison to other known stem birds, suggesting that olfaction was an important aspect of *Jeholornis* ecology. The digitally reconstructed scleral ring suggests a strongly diurnal habit, supporting the hypothesis that early-diverging birds were predominantly active during the day.

ADDITIONAL KEYWORDS: dentition – diurnality – Jehol Biota – neurocranium

INTRODUCTION

Jeholornithiformes is an early-diverging bird group from the Early Cretaceous Jehol Biota of China, retaining numerous primitive features, such as a long, bony tail (Zhou & Zhang, 2002; O'Connor *et al.*, 2012; Rauhut *et al.*, 2018). Among Aves, they are resolved by almost all phylogenetic analyses as being the earliest diverging Cretaceous stem bird lineages, crownward only to the Late Jurassic *Archaeopteryx* Meyer, 1861 from the Solnhofen Limestones in southern Germany (Zhou & Zhang, 2007; Zhou, 2014; O'Connor *et al.*, 2016, 2017; Wang *et al.*, 2019b, 2020b; Wang *et al.*, 2019a). Jeholornithiformes is the sister lineage of Pygostylia, a clade that includes the edentulous Confuciusornithiformes, *Sapeornis* Zhou & Zhang, 2002, in addition to the species-rich Enantiornithes and Ornithuromorpha (the lineage that gave rise to modern birds), with the last two of these clades together forming Ornithothoraces.

*Corresponding authors. E-mail: wangyan6696@lyu.edu.cn; han.hu@earth.ox.ac.uk

Approximately 100 specimens have been reported for *Jeholornis* Zhou & Zhang, 2002, with most specimens being referred to *Jeholornis* sp. (O'Connor *et al.*, 2018; Zheng *et al.*, 2020). Two species of *Jeholornis* are widely accepted as valid, *Jeholornis prima* Zhou, 2002 and *Jeholornis palmapenis* O'Connor, 2012, while the validity of *Jeholornis curvipes* Lefèvre, 2014 remains controversial (Zhou & Zhang, 2002; O'Connor *et al.*, 2012; Lefèvre *et al.*, 2014). However, whether the presence of maxillary dentition is diagnostic of *J. palmapenis* is questionable owing to the poor preservation of the maxillae in other published *Jeholornis* specimens. Besides *Jeholornis*, three other genera of Jeholornithiformes are variably regarded as valid: *Shenzhouraptor* Ji *et al.*, 2002, *Jixiangornis* Ji *et al*., 2002 and *Kompsornis* Wang *et al*., 2020 (Ji *et al.*, 2002a, b; Wang *et al.*, 2020a). The large collection of available *Jeholornis* specimens has been used to glean information regarding their tail plumage, stomach contents, sternal ossification and ventilatory apparatus (Ji *et al.*, 2002a, b; Zhou & Zhang, 2002, 2003; Gao & Liu, 2005; O'Connor *et al.*, 2012, 2013a, 2018; Lefèvre *et al.*, 2014; Zheng *et al.*, 2014, 2020; Wang *et al.*, 2020a). However, little information is available regarding the details of the cranial morphology, which is obscured by various factors, including the fragile nature of the cranial bones of birds, the crushed, two-dimensional (2D) preservation of most specimens from the Jehol deposits, and the fact that the cranial elements of these specimens are preserved in articulation, such that morphology is additionally obscured by overlaps.

Although the Jehol Biota provides some of the most important palaeontological insights into early bird evolution (Zhou & Wang, 2010; Zhou, 2014; Xu *et al.*, 2020), the anatomical and taxonomic knowledge of Jehol birds is far from complete. Few attempts have been made to provide comprehensive descriptions of the cranial morphology of Jehol birds, either 2D or three-dimensional (3D), with only some 2D descriptions for confuciusornithiforms and enantiornithines, and with limited 3D descriptions for *Sapeornis* and one juvenile enantiornithine (O'Connor & Chiappe, 2011; Elżanowski *et al.*, 2018; Wang *et al.*, 2019a, 2021; Hu *et al.*, 2020a). As the stem-most lineage of Cretaceous birds, a comprehensive study of the cranial anatomy of *Jeholornis* is particularly important for understanding early stages in the cranial transformation of birds. Cranial anatomical information is also crucial for understanding purported diagnostic characters relevant to the taxonomy of this lineage. Lastly, cranial morphology also potentially provides palaeobiological information relevant to understanding the ecology of *Jeholornis*.

Here, we provide a detailed cranial osteological description of *J. prima*, based primarily on the recently reported specimen STM 3-8 (Hu *et al.*, 2022; Fig. 1), with limited contributions from previously described jeholornithiforms (see Material and methods section). Although the skull of STM 3-8 is flattened, it is nearly complete, and the individual cranial elements are mostly preserved intact, with minimal crushing, allowing 3D reconstruction of the skull. This skull was included in recent geometric morphometric analyses of the cranium and mandible of fossil and extant birds. Together with 3D comparisons of the alimentary contents in extant birds, it helped to clarify the diet of *Jeholornis* as seasonally frugivorous rather than granivorous (Hu *et al.*, 2022), representing the earliest evidence for fruit consumption and probable seed dispersal in birds (Hu *et al.*, 2022). Key cranial morphologies of *Jeholornis* STM 3-8 were mentioned in the original paper, but a comprehensive description was not provided (Hu *et al.*, 2022). Here, we present a detailed anatomical description of the cranial morphology of *J. prima* based primarily on this specimen, including information regarding the morphology of the endocast for the first time. The exact dental arrangement of *Jeholornis* is clarified based on the information from STM 3-8 and confirmed by a large sample of specimens from the single largest collection of *Jeholornis* in the world, housed in the Shandong Tianyu Museum of Nature, China. Through analyses of the olfactory bulbs and the scleral ring, we also begin to understand the olfactory and visual capabilities of this taxon, thus greatly enriching our understanding of the palaeobiology of this important avian lineage.

MATERIAL AND METHODS

Jeholornis STM 3-8 was collected from the deposits of the Lower Cretaceous Jiufotang Formation at the Dapingfang locality near Chaoyang, Liaoning Province, China (He *et al.*, 2004), and was referred to *J. prima* by Hu *et al.* (2022). This study also includes data from *IVPP V13274* (*J. prima* holotype) (Zhou & Zhang, 2002), CDPC-02-04-001 (originally described as the holotype of *Jixiangornis orientalis* Ji, 2002) (Ji *et al.*, 2002b), LPM 0193 (originally described as the holotype of *Shenzhouraptor sinensis* Ji, 2002) (Ji *et al.*, 2002a), IVPP V13553 (*J. prima*) (Zhou & Zhang, 2003), *SDM 20090109.1/2* (*J. palmapenis* holotype) (O'Connor *et al.*, 2012), YFGP-yb2 (originally described as the holotype of *J. curvipes*) (Lefèvre *et al.*, 2014), AGB-6997 (originally described as the holotype of *Kompsornis longicaudus* Wang, 2020) (Wang *et al.*, 2020a) and undescribed jeholornithiforms housed in STM (Supporting Information, Table S1; Zheng *et al.*, 2014). Anatomical terminology primarily follows Baumel & Witmer (1993), using the English equivalents of the latinized osteological features.

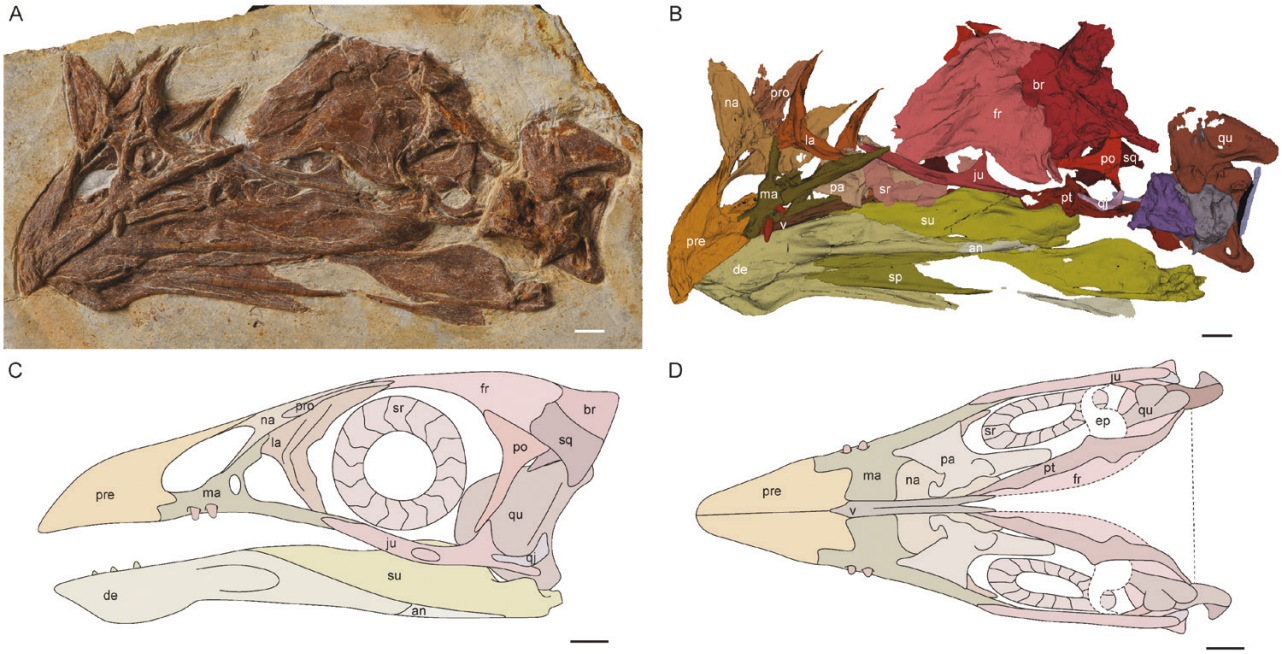

Figure 1. Photograph (A), left view of the three-dimensionally reconstructed skull (B) and lateral (C) and ventral (D) views of the two-dimensional cranial reconstruction of *Jeholornis* STM 3-8 (following Hu *et al.*, 2022). Scale bars: 5 mm. Abbreviations: an, angular; br, braincase; de, dentary; ep, ectopterygoid; fr, frontal; ju, jugal; la, lacrimal; ma, maxilla; na, nasal; pa, palatine; pre, premaxilla; po, postorbital; pro, preorbital ossification; pt, pterygoid; qj, quadratojugal; qu, quadrate; sp, splenial; sq, squamosal; sr, scleral ring; su, suangular; v, vomer. Dashed lines indicate the elements not preserved but suspected to exist.

The olfactory bulb ratio was calculated using linear measurements of the olfactory bulbs and forebrain in the software FIJI, following Zelenitsky *et al.* (2011).

INSTITUTIONAL ABBREVIATIONS

AGB, Anhui Geological Museum, Hefei, Anhui, China; CDPC, Changzhou Dinosaur Park of China, Changzhou, China; IVPP, Institute of Vertebrate Paleontology and Paleoanthropology, Chinese Academy of Sciences, Beijing, China; LPM, Liaoning Paleontology Museum, Shenyang, Liaoning, China; SDM, Shandong Museum, Jinan, China; STM, Shandong Tianyu Museum of Nature, Shandong, China; YFGP, Yizhou Fossil and Geology Park, Yizhou, China.

RESULTS

CRANIAL OSTEOLOGY OF *JEHOLORNIS*

Premaxilla

The premaxillae are complete in STM 3-8 (Fig. 2A–F). They are edentulous, as reported in previous publications (Zhou & Zhang, 2002, 2003; Lefèvre *et al.*, 2014), and their external surfaces are marked by several nutrient foramina. No pits are present to receive the dentary teeth, which is different from the condition present in *Ichthyornis* Marsh, 1873 (Field *et al.*, 2018). The tip of the corpus forms a ventral projection, suggesting that the tip of the beak might have been slightly hooked. Caudal to the rostral 'hook', the ventral margin of the premaxillary corpus is straight. The relative level of the ventral projection of this rostral 'hook' varies among previously reported specimens, being absent in *Jeholornis* YFGP-yb2 and exaggerated relative to STM 3-8 in *Kompsornis* AGB-6997 (Lefèvre *et al.*, 2014; Wang *et al.*, 2020a). This is interpreted here as attributable to variation in preservation, but further studies are needed to exclude the possibility of intraspecific variation confidently. The premaxillary corpora are fused, whereas the frontal processes are separated (Hu *et al.*, 2022).

The frontal (nasal) process of the premaxilla is relatively short and therefore does not contact the frontal but instead articulates distally with the dorsal surface of the nasal, as in other non-ornithothoracine stem birds (e.g. *Archaeopteryx* and *Sapeornis*; Rauhut, 2014; Kundrát *et al.*, 2018; Hu *et al.*, 2020a) apart from *Confuciusornis* Hou *et al.*, 1995 (Chiappe *et al.*, 1999; Elżanowski *et al.*, 2018; Wang *et al.*, 2019a). This is evidenced by the extension level of the articular facet present in the frontal process of the premaxilla. The maxillary process of the premaxilla is short and

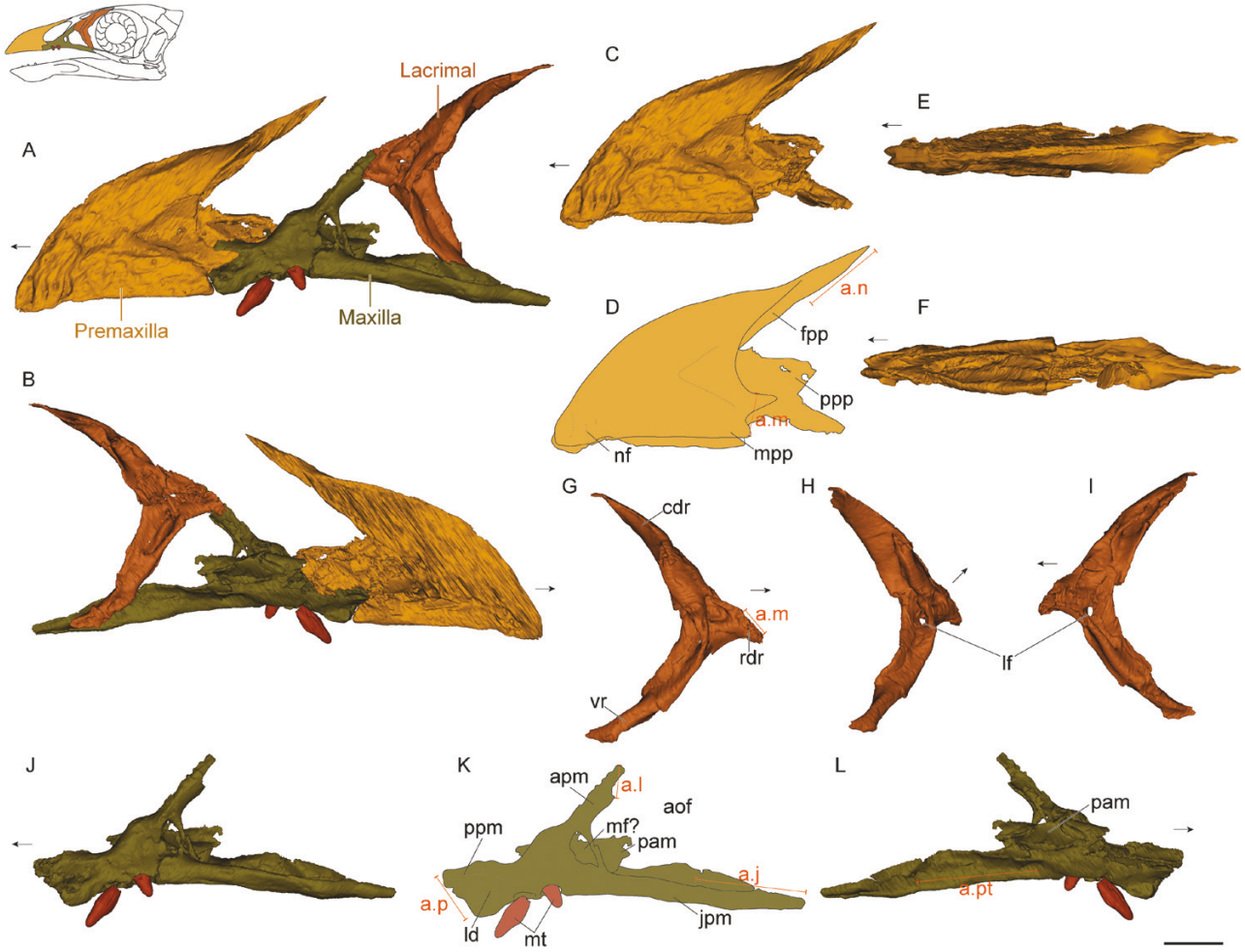

Figure 2. Three-dimensional snapshots of rostral cranial elements of *Jeholornis* STM 3-8: lateral (A) and medial (B) views of the articulated left premaxilla, maxilla and lacrimal; lateral view (C), lateral line drawing (D), dorsal view (E) and ventral view (F) of the fused premaxillae; lateral (G), caudolateral (H) and medial (I) views of the right lacrimal; lateral view (J), lateral line drawing (K) and medial view (L) of the left maxilla. Scale bar: 5 mm. Arrows indicate the rostral direction. Labels for articular facets are in red. Abbreviations: a.j, jugal articulation; a.l, lacrimal articulation; a.m, maxilla articulation; a.n, nasal articulation; aof, antorbital fenestra; a.p, premaxilla articulation; a.pt, palatine articulation; apm, ascending process of maxilla; cdr; caudodorsal ramus of lacrimal; fpp, frontal process of premaxilla; jpm, jugal process of maxilla; ld, lateral depression of maxilla to receive the maxillary process of premaxilla; lf, lacrimal foramen; mf?, potential maxillary fenestra; mpp, maxillary process of premaxilla; mt, maxillary teeth; nf, nutrient foramina; pam, palatal process of maxilla; ppm, premaxillary process of maxilla; ppp, palatal process of premaxilla; rdr, rostrodorsal ramus of lacrimal; vr, ventral ramus of lacrimal.

articulates medially with the premaxillary process of the maxilla (Fig. 2A, B). It appears to be step-like, with the dorsal margin extending farther caudally than the ventral margin. The palatal process is crushed mediolaterally but could still be distinguished from the maxillary process in the 3D reconstruction.

Maxilla

The maxillae in *Jeholornis* STM 3-8 are well preserved, being almost in articulation with the premaxillae and the lacrimals (Fig. 2A, B, J–L). The premaxillary process bears a lateral depression that receives the dorsal part of the maxillary process of premaxilla. The jugal process is slender, being half of the dorsoventral height of the premaxillary process and more than twice its length. A shallow groove is present along the medial surface of the jugal process, indicating extensive contact area with the palatine, similar to *Archaeopteryx* (Mayr *et al.*, 2007). The medial surface of the maxilla is rarely visible among Mesozoic bird specimens, precluding further comparisons. Although

the palatal process is mostly crushed, it seems that it was sheet-like and well developed, and therefore most probably contacted the vomer, similar to the Late Cretaceous enantiornithine *Gobipteryx* Elżanowski, 1974 and the ornithuromorph *Ichthyornis* (Chiappe *et al.*, 2001; Field *et al.*, 2018), the only other Mesozoic birds in which the morphology of the palatal process of the maxilla is known so far. A dorsoventrally elongate oval fenestra is present between the jugal process and the ascending process in *Jeholornis*, being enclosed caudally by a thin, bony bar. We identify this tentatively as the maxillary fenestra (Witmer, 1997). However, it is unclear whether it is homologous with the maxillary fenestra or promaxillary fenestra of non-avian theropods and *Archaeopteryx* (Witmer, 1997; Barsbold & Osmólska, 1999; Xu & Wu, 2001; Mayr *et al.*, 2007; Rauhut, 2014; Rauhut *et al.*, 2018) or with the accessory fenestra present in the enantiornithine bird *Pengornis* Zhou, Clarke & Zhang, 2008 (O'Connor & Chiappe, 2011).

Two alveoli are present in the maxilla. Two teeth are preserved in the left maxilla, and another two similar-sized teeth are dislocated beside the right maxilla. The maxillary teeth are straight and subconical, with blunt crowns and an expanded root.

Lacrimal

Both lacrimals are well preserved in articulation with the maxillae in *Jeholornis* STM 3-8 (Fig. 2A, B, G–I). The rostrodorsal ramus is remarkably short, approximately one-quarter the length of the long caudodorsal ramus. This differs from most other Early Cretaceous birds and non-avian theropods (e.g. *Archaeopteryx* and *Sinornithosaurus* Xu, Wang & Wu, 1999; Xu & Wu, 2001; Rauhut, 2014; Kundrát *et al.*, 2018; Rauhut *et al.*, 2018), in which the rostrodorsal ramus is long and the caudodorsal ramus short. The ventral ramus is caudally recurved in *Jeholornis*, such that the caudal margin formed by the ventral and caudodorsal processes is concave, forming the rostral/rostrodorsal margin of the orbit. This is similar to the morphology in more crownward birds (e.g. the Late Cretaceous ornithurine bird *Ichthyornis*), although the rostrodorsal ramus is even more strongly reduced in *Ichthyornis* and does not contact the maxilla, unlike in *Jeholornis* (Field *et al.*, 2018). The lacrimal morphology of *Jeholornis* also contrasts with the morphology of most other Early Cretaceous birds and non-avian theropods, in which the ventral ramus is almost perpendicular to the ventral margin of the skull or is inclined cranially (Wang *et al.*, 2021). The lacrimal of the confuciusornithiforms appears to be slender and reduced, also presenting a short or totally absent rostrodorsal ramus and slightly caudally recurved ventral ramus (Elżanowski *et al.*, 2018; Wang & Zhou, 2018; Wang *et al.*, 2019a), potentially similar to *Jeholornis*. However, owing to the potential uncertainty from 2D preservation of currently published skulls of confuciusornithiforms, 3D data are needed to confirm this in future analyses.

Disarticulation prevents detailed reconstruction of articulations between the lacrimal, the nasal and the preorbital ossification in *Jeholornis* STM 3-8. The ventral ramus of the lacrimal is interpreted as contacting the jugal process of the maxilla and, potentially, might have contacted the rostral tip of the jugal, whereas the lacrimal contacts the jugal in other theropods (Xu & Wu, 2001; Rauhut, 2014; Kundrát *et al.*, 2018; Rauhut *et al.*, 2018). The caudal margin of the lacrimal, which forms the cranial margin of the orbit, is remarkably excavated, and the excavation extends across both the ventral and caudodorsal processes. A lacrimal foramen lies within the centre of the excavation, entering medially into the main body of the lacrimal at around its mid-height, at the junction of the ventral ramus and the caudodorsal ramus. The size and central position of this foramen resemble the condition in *Ichthyornis* (Field *et al.*, 2018), although the lacrimal of *Ichthyornis* differs in lacking the rostrodorsal ramus and thus the contact with the maxilla. In contrast, this foramen is much smaller and penetrates lateromedially in enantiornithine IVPP V12707, which also lacks any excavation on the lacrimal on the rostral orbit margin of the lacrimal (Wang *et al.* 2021). This contrasts with the craniocaudal extension of the lacrimal foramen in *Jeholornis*.

Nasal

The left nasal is well preserved (Fig. 3A, B). The nasal corpus is mediolaterally broad, similar to *Sapeornis* (Hu *et al.*, 2019, 2020a) but unlike the more elongated condition present in *Archaeopteryx* (Mayr *et al.*, 2007; Rauhut, 2014; Kundrát *et al.*, 2018), confuciusornithiforms (Elżanowski *et al.*, 2018; Wang *et al.*, 2019a) and enantiornithines (O'Connor & Chiappe, 2011). Both the premaxillary and the maxillary processes are delicate and sharply tapered rostrally. The premaxillary process is slightly longer than the maxillary process, and the deflections of both processes in the left nasal are taphonomic, resulting from crushing between the right nasal and left lacrimal. The premaxillary process does not extend to the base of the frontal process of the premaxilla, therefore leaving the premaxilla to form most of the rostrodorsal margin of the external naris. This is different from the condition in *Archaeopteryx*, in which the premaxillary process is substantially longer than the maxillary process and forms part of the dorsal–rostrodorsal margin of the external naris (Rauhut, 2014; Kundrát *et al.*, 2018).

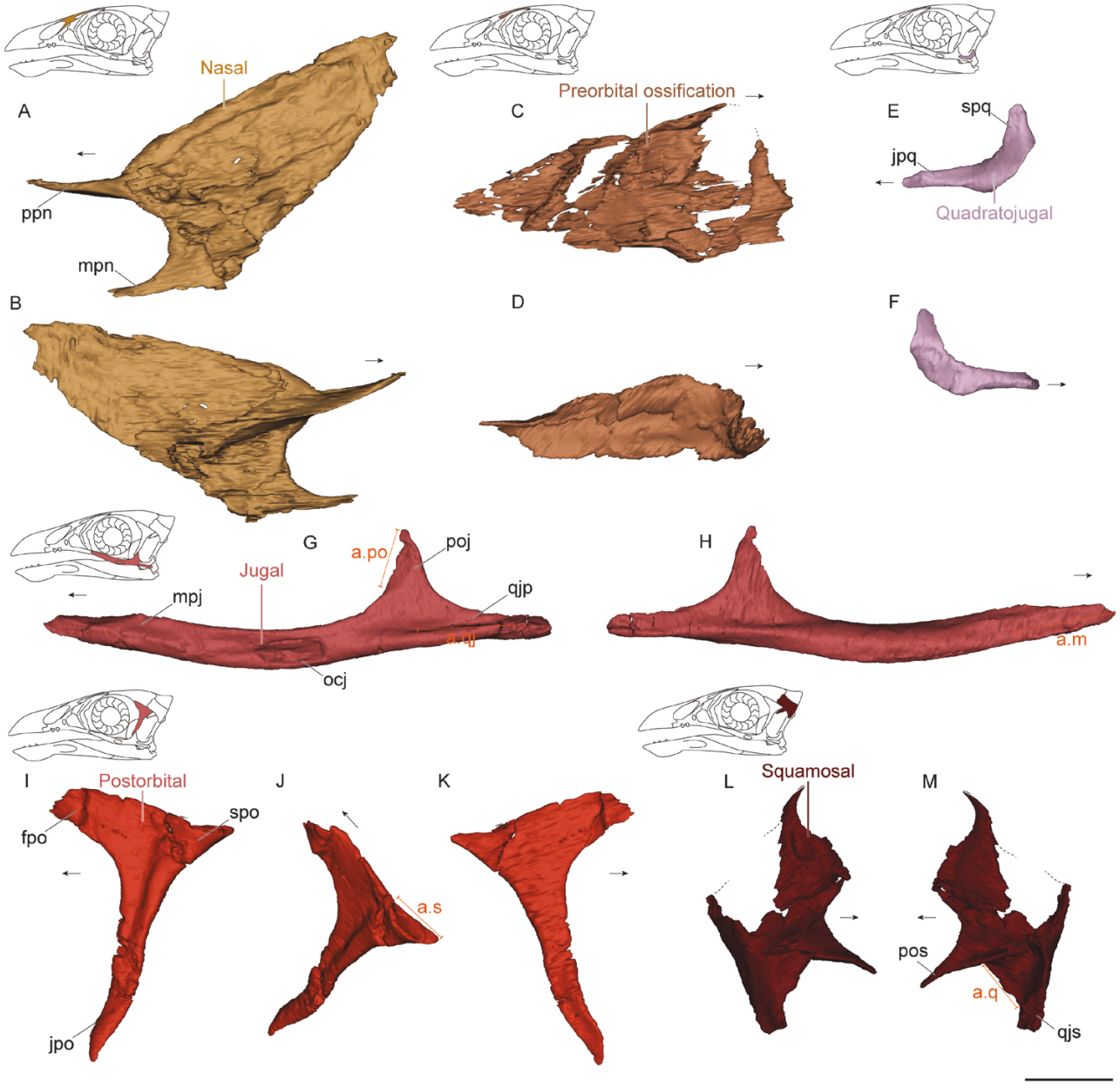

Figure 3. Three-dimensional snapshots of lateral and dorsal cranial elements of *Jeholornis* STM 3-8: dorsal lateral (A) and ventromedial (B) views of the left nasal; dorsal views of the right (C) and left (D) preorbital ossification; lateral (E) and medial (F) views of the left quadratojugal; lateral (G) and medial (H) views of the left jugal; lateral (I), laterocaudal (J) and medial (K) views of the left postorbital; lateral (L) and medial (M) views of the right squamosal. Scale bar: 5 mm. Arrows indicate the rostral direction. Labels for articular facets are in red. Dashed lines indicate broken margins. Abbreviations: a.m, maxilla articulation; a.po, postorbital articulation; a.q, quadrate articulation; a.qj, quadratojugal articulation; a.s, squamosal articulation; fpo, frontal process of postorbital; jpo, jugal process of postorbital; jpq, jugal process of quadratojugal; mpj, maxillary process of jugal; mpn, maxillary process of nasal; ocj, oval concavity of jugal; poj, postorbital process of jugal; pos, postorbital process of squamosal; ppn, premaxillary process of nasal; qjp, quadratojugal process of jugal; qjs, quadratojugal process of squamosal; spo, squamosal process of postorbital; spq, squamosal process of quadratojugal.

The maxillary process of the premaxilla of *Jeholornis* is also relatively short and does not extend to the base of the ascending process of the maxilla, therefore not contacting the premaxilla. This leaves the maxilla to form the caudoventral margin of the external naris, similar to *Archaeopteryx* (Rauhut, 2014).

Preorbital ossification

Specimen STM 3-8 preserves a mysterious pair of sheet-like elements previously referred to as 'preorbital ossifications' (Fig. 3C, D; Hu *et al.*, 2022), which might represent prefrontals based on their overall shape and location. This is supported by their location almost parallel to the craniodorsal process of the lacrimal, which rules out identification as the ectethmoid, especially considering that other rostral elements are mostly preserved *in situ*. If this element is the prefrontal, it differs from the prefrontals of all other pennaraptorans so far, which are strongly reduced or absent, being typically smaller than the nasal (e.g. in *Archaeopteryx* and *Sinornithosaurus*; Xu & Wu, 2001; Rauhut *et al.*, 2018). This could suggest that an unfused, expanded prefrontal might be a derived feature of *Jeholornis* and challenges the hypothesis based on the embryonic observations that the prefrontal fused to form the caudodorsal ramus of the lacrimal in all birds (Smith-Paredes *et al.*, 2018). If correctly identified, this suggests that a broad prefrontal co-exists with a lacrimal with a well-developed caudodorsal process in *Jeholornis*. However, owing to the lack of available comparisons of any similar ossifications among non-avian dinosaurs and birds, we cannot exclude the possibility that this bone represents some other element that is rarely preserved or developed in Mesozoic birds. For example, the preorbital ossification described here could be a palpebral, although we consider this to be much less likely owing to its preserved location, close to the midline of the skull.

Jugal

Only the left jugal is preserved in STM 3-8 (Fig. 3G, H). The maxillary process is as slender as the jugal process of the maxilla, similar to the jugal of *Archaeopteryx* (Elżanowski & Wellnhofer, 1996; Kundrát *et al.*, 2018; Rauhut *et al.*, 2018) but in contrast to the relatively more robust condition in *Sapeornis* (Hu *et al.*, 2020a). The rostral quarter of the maxillary process is slightly constricted and bears a depression in the distal end of the dorsal margin, defining the articulation with the maxilla. The articulation between the jugal and the maxilla is much shorter than in *Sapeornis*, in which the maxilla extends caudally almost to the base of the postorbital bar (Hu *et al.*, 2020a). An oval concavity is present centrally on the lateral surface of the maxillary process. A similar depression is also present in *Archaeopteryx*, although in a more rostral position (Mayr *et al.*, 2007; Rauhut, 2014), but is absent in most other Mesozoic birds (e.g. *Sapeornis*, *Ichthyornis* and enantiornithines; Wang & Hu, 2017; Field *et al.*, 2018; Hu *et al.*, 2020a). The quadratojugal process of the jugal of *Jeholornis* lacks the notch present in *Sapeornis* and many non-avian theropods, which is also absent in known enantiornithines but possibly present in *Ichthyornis* (Rauhut, 2003; Xu *et al.*, 2015; Wang & Hu, 2017; Field *et al.*, 2018; Hu *et al.*, 2020b). Because of this, the quadratojugal of *Jeholornis* articulates with the dorsolateral surface of the quadratojugal process of the jugal, differing from the wedge-like articulation seen in *Sapeornis* and other Mesozoic theropods (e.g. *Linheraptor* Xu *et al.*, 2015; Xu *et al.*, 2015; Hu *et al.*, 2020a). The postorbital process of the jugal of *Jeholornis* is triangular with a broad base and is dorsally oriented. This contrasts with the caudodorsal orientation seen in *Archaeopteryx* and *Sapeornis* (Mayr *et al.*, 2007; Rauhut, 2014; Kundrát *et al.*, 2018; Hu *et al.*, 2020a). A shallow impression on the rostrolateral surface of the postorbital process defines the articulation with the postorbital, indicating the presence of a complete postorbital bar in *Jeholornis*.

Quadratojugal

The left quadratojugal is complete, but slightly disarticulated from the jugal (Fig. 3E, F). The jugal process is twice as long as the squamosal process and is more slender; both are bluntly tapered. The ventromedial surface of the jugal process contacts the jugal, in contrast to the inserting articulation with the caudal notch of the jugal in *Sapeornis* and most non-avian theropods (Xu *et al.*, 2015; Hu *et al.*, 2020a). The squamosal process is reduced and does not contact the squamosal dorsally, similar to the condition in other Mesozoic birds, including *Archaeopteryx*, *Sapeornis* and various others (e.g. *Rapaxavis pani* Morschhauser *et al.*, 2009 and *Cruralispennia multidonta* Wange *et al.*, 2017; Mayr *et al.*, 2007; O'Connor *et al.*, 2011; Rauhut, 2014; Wang *et al.*, 2017b; Hu *et al.*, 2020a).

Postorbital

The left postorbital is completely preserved and the right is broken in STM 3-8 (Fig. 3I–K). The postorbital is triradiate and more robust than that of *Archaeopteryx* (Kundrát *et al.*, 2018; Rauhut *et al.*, 2018; Hu *et al.*, 2020a). The jugal process is long and tapers ventrally, extending most of the skull height ventrally, and therefore forming most of the postorbital bar. In contrast, one specimen of *Archaeopteryx* preserves a slightly longer jugal process (Rauhut *et al.*, 2018), whereas others preserve a jugal process almost equal in length to the other processes (Kundrát *et al.*, 2018). The elongate jugal process of *Jeholornis* more closely resembles the condition in some enantiornithines (e.g. *Longusunguis* Wang *et al.*, 2014 and enantiornithines LP4450 and IVPP V12707). However, it is much more robust than that of some other enantiornithines (Sanz *et al.*, 1997; Hu *et al.*, 2020b; Zhou *et al.*, 2008). The

squamosal process of the postorbital of *Jeholornis* is short, less than half the length of the frontal process, and has a sharply tapered end, whereas this process is longer in *Sapeornis* and *Archaeopteryx* (Rauhut *et al.*, 2018; Hu *et al.*, 2020a). The dorsal surface of the squamosal process bears a concave facet for articulation with the squamosal.

Squamosal

Both squamosals are preserved, although only the right is complete in STM 3-8 (Fig. 3L, M). The squamosal is not fused to the braincase, similar to the condition in non-avian theropods, *Archaeopteryx* and enantiornithines (e.g. LP4450 and IVPP V12707; Elżanowski & Wellnhofer, 1996; Sanz *et al.*, 1997; Rauhut, 2003; Norman *et al.*, 2004; Xu *et al.*, 2015; Rauhut *et al.*, 2018; Wang *et al.*, 2021). The rarity with which squamosals are preserved in other stem birds complicates interpretation of the morphology seen in *Jeholornis*. However, the concavity in the medial surface of this bone fits the otic process of the quadrate, and thus could be interpreted as the quadrate cotyle of the squamosal, supporting our identification of this element as a squamosal. The triangular, sharply tapered, rostroventrally directed process is identified as the postorbital process, resembling that in enantiornithine IVPP V12707 (Wang *et al.*, 2021), and contrasts with the forked condition in *Archaeopteryx* (Elżanowski & Wellnhofer, 1996; Kundrát *et al.*, 2018). The ventrally oriented quadratojugal process is short, with a blunt ventral margin, not contacting the quadratojugal. This suggests that the loss of the quadratojugal–squamosal contact might have evolved independently in *Jeholornis* and in ornithurines, but remained present in at least some enantiornithines (e.g. IVPP 12707) [although it also could have been regained secondarily as a derived feature (Wang *et al.*, 2021)]. It cannot be determined whether the dorsal portion is complete, hence the shape of the parietal and the paroccipital processes of the squamosal remain uncertain.

Quadrate

Both quadrates are almost completely preserved (Fig. 4A–C). The shaft of the quadrate extends from the otic process dorsally to the lateral condyle caudoventrally. The orbital process is broad and lateromedially thin, resembling that of *Archaeopteryx* (Rauhut *et al.*, 2018), *Sapeornis* (Hu *et al.*, 2020a) and known enantiornithines [e.g. *Zhouornis* Zhang *et al.*, 2013 (Zhang *et al.*, 2013) and *Pterygornis* Wang *et al.*, 2014 (Wang *et al.*, 2015)], and differs from the narrow and rostrally projecting condition in *Ichthyornis* and crown birds, including the Late Cretaceous *Asteriornis* Field *et al.*, 2020 (Elżanowski & Stidham, 2010; Field *et al.*, 2018, 2020). The otic process is plesiomorphically single headed, as in *Sapeornis* and enantiornithines (Wang *et al.*, 2015, 2021; Hu *et al.*, 2020a), but differing from the divided otic capitulum and squamosal capitulum in neognaths, including *Asteriornis* (Field *et al.*, 2020). A dorsoventrally oriented longitudinal ridge is present caudally on the medial surface of the otic process, similar to the condition in *Sapeornis* and enantiornithines (Zhang *et al.*, 2013; Wang *et al.*, 2015; Hu *et al.*, 2020a), defining the caudal margin of a gentle excavation on the medial surface of the orbital process. The lateral surface is also excavated by a similar dorsoventrally oriented longitudinal ridge, but it cannot be determined whether this is attributable to the lateromedially crushed preservation of the orbital process. No pneumatic foramen is observed, different from the condition in most modern birds and Late Cretaceous ornithurines (e.g. *Ichthyornis* and *Asteriornis*; Elżanowski & Stidham, 2010; Field *et al.*, 2018, 2020). However, two potential pneumatic recesses could be identified on the lateral surface of the quadrate in *Jeholornis*. Both the lateral and medial condyles are of a similar size and project caudally, defining a concave caudal margin for the quadrate.

Frontal

The frontals are tightly articulated with each other in STM 3-8, but not entirely fused, with the interfrontal suture clearly visible (Fig. 4D, E), similar to the condition observed in other *Jeholornis* specimens (Lefèvre *et al.*, 2014). The rostral half is narrow, half the mediolateral width of the expanded caudal half, along which a supraorbital rim is well developed laterally. This rim, together with the orbital margin of the frontal, form the dorsal and the medial walls of the orbit.

Parietal and braincase

The parietals and the braincase are crushed together, preventing segmentation of the individual elements (Fig. 4F–H). The parietals are in tight contact medially, similar to the frontals. Owing to poor preservation, it cannot be determined whether they are entirely fused, as in some non-avian theropods (Clark *et al.*, 2002; Yin *et al.*, 2018), or if the interparietal suture still exists, as in *Archaeopteryx* (Rauhut, 2014; Kundrát *et al.*, 2018; Rauhut *et al.*, 2018). The nuchal crest is straight and forms a well-developed ridge. The sagittal crest is absent in the conjoined parietals, but a supratemporal fossa reaching the dorsal portion of the parietal is still present. It is probable that the elements forming the occiput are either fused or sutured with each other, although this area is strongly crushed, preventing

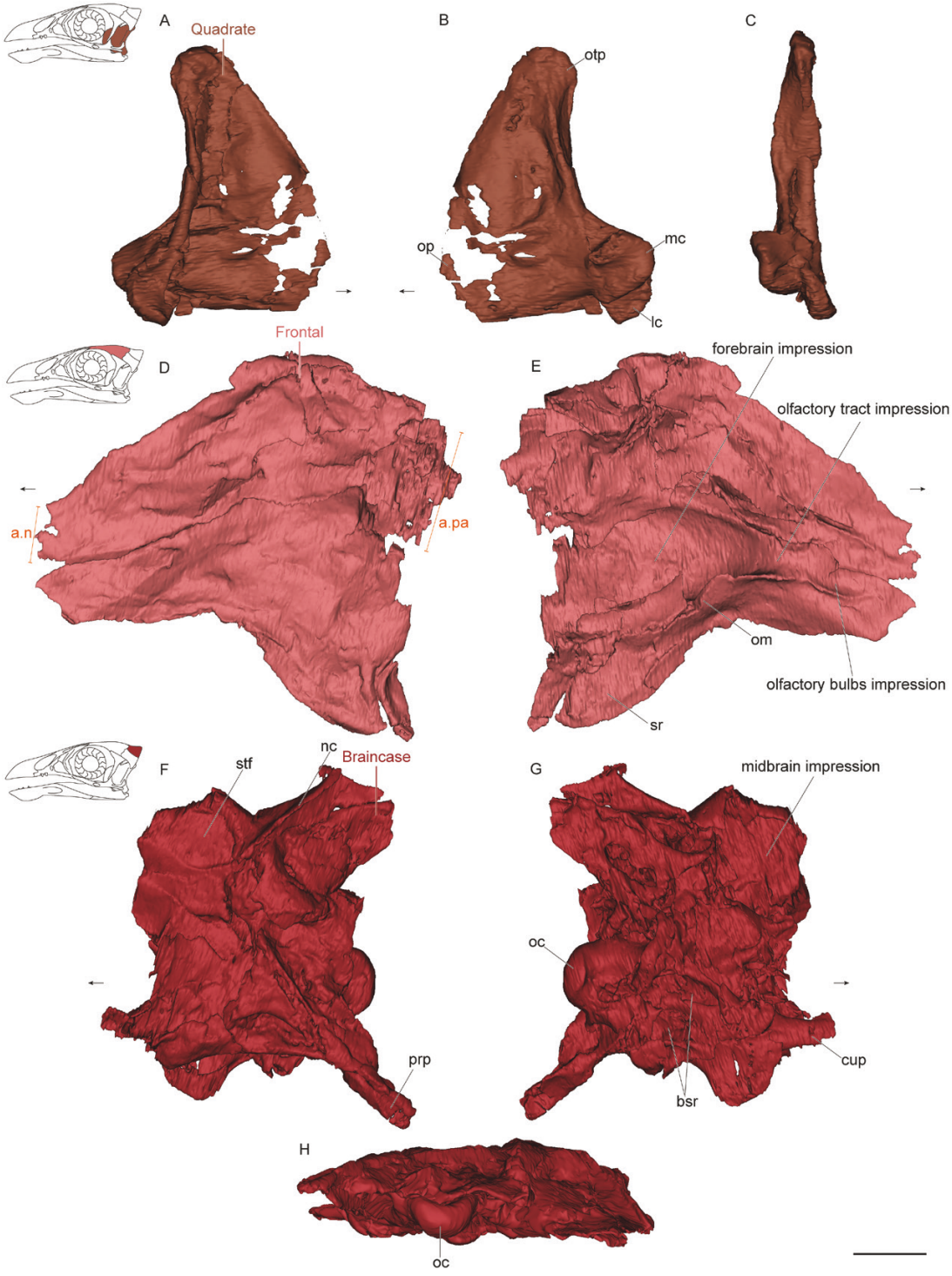

Figure 4. Three-dimensional snapshots of the quadrate and skull roof of *Jeholornis* STM 3-8: lateral (A), medial (B) and caudal (C) views of the right quadrate; dorsal (D) and ventral (E) views of the frontals; dorsal (F), ventral (G) and caudal (H) views of the braincase. Scale bar: 5 mm. Arrows indicate the rostral direction. Labels for articular facets are in red. Dashed lines indicate broken margins. Abbreviations: a.n, nasal articulation; a.pa, parietal articulation; bsr, basisphenoid recess; cup, cultriform process; lc, lateral condyle of quadrate; mc, medial condyle of quadrate; nc, nuchal crest; oc, occipital condyle; op, orbital process of quadrate; om, obital margin; otp, otic process of quadrate; prp, paroccipital process; sr, supraorbital rim; stf, supratemporal fossa. Labels of neurocranial elements are not abbreviated.

detailed observations. The paroccipital process is lateroventrally and somewhat caudally oriented and similar in length to *Archaeopteryx* (Kundrát *et al.*, 2018; Rauhut *et al.*, 2018). The occipital condyle is rounded and bears a shallow depression on the caudoventral surface. Two rostrocaudally elongate fossae are identified as the basisphenoid recesses rostroventral to the occipital condyle visible in ventral view. The cultriform process is dorsally concave and slightly restricted in the distal end. We refrain from describing other features owing to the crushed preservation, which makes the braincase morphology difficult to interpret.

Endocast

The braincase of *Jeholornis* STM 3-8 is partly crushed and deformed, preventing a full endocranial reconstruction. Nevertheless, a mosaic of derived and plesiomorphic characters can be inferred from the dorsal surface of the endocast, defined by the ventral surface of the skull roof elements (Fig. 4) (Fabbri *et al.*, 2017; Beyrand *et al.*, 2019; Watanabe *et al.*, 2019).

Ventrolateral shift of the midbrain endocast is clearly present (Fig. 4), as observed in *Archaeopteryx* and other non-avian paravians (Alonso *et al.*, 2004; Balanoff *et al.*, 2013). The forebrain endocast is expanded, which is a plesiomorphic condition shared among paravians (Balanoff *et al.*, 2013; Fabbri *et al.*, 2017; Beyrand *et al.*, 2019). The optic bulbs are laterally placed in comparison to more basal theropods, but not ventrally shifted as in modern birds (Fabbri *et al.*, 2017; Beyrand *et al.*, 2019). The ventral surfaces of the frontals indicate broad, well-developed olfactory bulbs, as in non-avian dinosaurs and *Archaeopteryx*. The olfactory tracts are mediolaterally wide and cranially elongated, contrary to modern birds (Balanoff *et al.*, 2013; Fabbri *et al.*, 2017; Beyrand *et al.*, 2019), although they are relatively shorter in comparison to other non-avian coelurosaurs, such as tyrannosauroids, dromaeosaurids and troodontids (Balanoff *et al.*, 2013; Fabbri *et al.*, 2017; Beyrand *et al.*, 2019).

Vomer

The vomer is completely preserved (Figs 5A, B, 6), although the pterygoid rami are slightly broken and distorted. The vomer is partly fused along approximately the one-quarter rostral portion, where the fused part is dorsoventrally arched such that its ventral surface is convex. Shallow impressions are located cranially on the ventral surface and are identified as the articular facets with the maxilla and, possibly, also the premaxilla. This indicates a dorsoventrally overlapping contact between the vomer and maxilla/premaxilla, resulting in limited cranial kinesis, similar to *Sapeornis*, enantiornithine IVPP V12707, non-avian dinosaurs and palaeognathous birds, but different from neognaths, in which the vomer contacts the maxillae more laterally (Tsuihiji *et al.*, 2014; Hu *et al.*, 2019, 2020a; Wang *et al.*, 2021). The unfused caudal portion of the vomers diverges into two caudal flanges (pterygoid rami) that are much longer than the fused rostral portion (Hu *et al.*, 2022) and proportionally much longer than the pterygoid rami of *Archaeopteryx* (Elżanowski & Wellnhofer, 1996). The vomers of *Jeholornis* lack the leaf-like caudodorsal process seen at the end of the pterygoid ramus in *Sapeornis* and some non-avian theropods (e.g. *Sinovenator*; Hu *et al.*, 2020a), which is also absent in *Archaeopteryx* and enantiornithines (e.g. *Gobipteryx*; Elżanowski & Wellnhofer, 1996; Chiappe *et al.*, 2001; Hu *et al.*, 2020a). Instead, the middle portions of the pterygoid rami are dorsoventrally expanded, possibly to accept the pterygoids or the parasphenoid rostrum. A shallow impression on the lateral surface of the dorsal expansion is interpreted as the palatine articulation, similar to the condition in the Late Cretaceous enantiornithine *Gobipteryx* (Chiappe *et al.*, 2001). The only Early Cretaceous enantiornithine bird preserving relatively complete vomer morphology, IVPP V12707, is immature and lacks cranial fusion, preventing unambiguous comparisons (Wang *et al.*, 2021).

Palatine

Both palatines are complete in STM 3-8 (Figs 5E, F, 6), preserved between the maxillae, and their morphology confirms identification of the palatine in the previously described *J. palmapenis SDM 20090109.1/2* (O'Connor *et al.*, 2012; Fig. 7). The palatine resembles that of *Archaeopteryx*, being unreduced and mediolaterally broad between the jugal process and the choanal process (Mayr *et al.*, 2007). In *SDM 20090109.1/2*, the base of the choanal process is perforated by a foramen (O'Connor *et al.*, 2012), although whether this derives from preservation cannot be determined. The margin between the maxillary process and jugal process is straight, thus the jugal process is almost triangular. The jugal process connects the palatal complex and the lateral cranium and is therefore important for evaluating the degree of possible cranial kinesis. This process is well developed in non-avian dinosaurs (Witmer, 1997; Tsuihiji *et al.*, 2014; Hu *et al.*, 2020a) and entirely reduced in crown birds and in known Late Cretaceous avian taxa, including the ornithuromorphs *Hesperornis* Marsh, 1872 and *Ichthyornis* and the enantiornithine *Gobipteryx* (Elżanowski, 1991; Chiappe *et al.*, 2001; Field *et al.*, 2018). The condition in the Early Cretaceous enantiornithines and ornithuromorphs is unclear because only few,

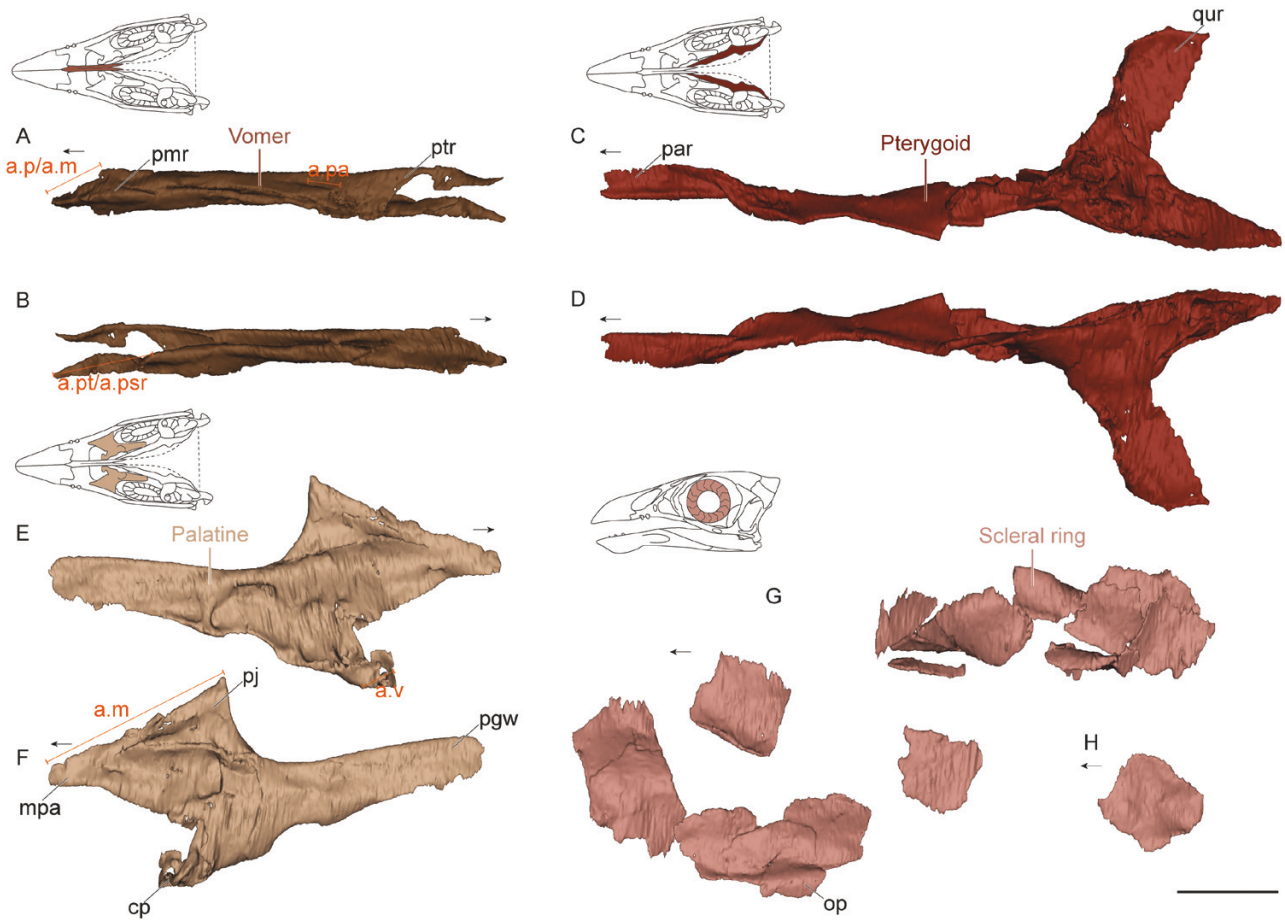

Figure 5. Three-dimensional snapshots of the palatal elements and scleral ring of *Jeholornis* STM 3-8: ventral (A) and dorsal (B) views of the vomer; medial (C) and lateral (D) views of the right pterygoid; ventral (E) and dorsal (F) views of the right palatine; left view of the scleral ring (G) and the scleral bone (H). Scale bar: 5 mm. Arrows indicate the rostral direction. Labels for articular facets are in red. Abbreviations: a.m, maxilla articulation; a.pa, palatine articulation; a.psr, parasphenoid rostrum articulation; a.pt, pterygoid articulation; a.v, vomer articulation; cp, choanal process; mpa, maxillary process of palatine; op, overplate; par, palatine ramus of pterygoid; pgw, pterygoid wing; pj, jugal process of palatine; pmr, premaxillary ramus of vomer; ptr, pterygoid ramus of vomer; qur, quadrate ramus of pterygoid.

ambiguously identified palatines are preserved (Xu *et al.*, 2021). Based on the condition in *Archaeopteryx* and *Jeholornis*, we tentatively interpret the lack of a jugal process in the palatine of *Sapeornis* as a preservational artefact (Hu *et al.*, 2019, 2020a) and suggest that all non-ornithothoracine birds are likely to have possessed a plesiomorphic, nearly akinetic palate that contacted the lateral cranium tightly. The jugal process of the palatine mostly contacts the maxilla but also contacts the rostral tip of the jugal in *Archaeopteryx* (Mayr *et al.*, 2007). However, based on the relative preserved position of the palatine, maxilla and jugal in STM 3-8, it is highly possible that the jugal process of the palatine only contacted the maxilla in *Jeholornis* (Hu *et al.*, 2022). This interpretation is also consistent with the fact that the maxilla extends farther caudally in *Jeholornis* than it does in *Archaeopteryx* (Mayr *et al.*, 2007). The medially hooked choanal process of the palatine articulates with the vomer medially, forming the caudal margin of the internal naris. The pterygoid wing of the palatine is long and slender, approximately half the maximum width of the palatine and forming more than half of its total length. Its caudal end is bluntly tapered, with straight lateral and medial margins. However, its caudal articulation with the pterygoid is unclear owing to the disarticulation.

Pterygoid

Both pterygoids are preserved in STM 3-8 but strongly crushed (Figs 5C, D, 6). Although most morphologies are ambiguous, this element is elongate, and a flange ventrally developed along most of the palatine process indicates the presence of an ectopterygoid (Hu *et al.*,

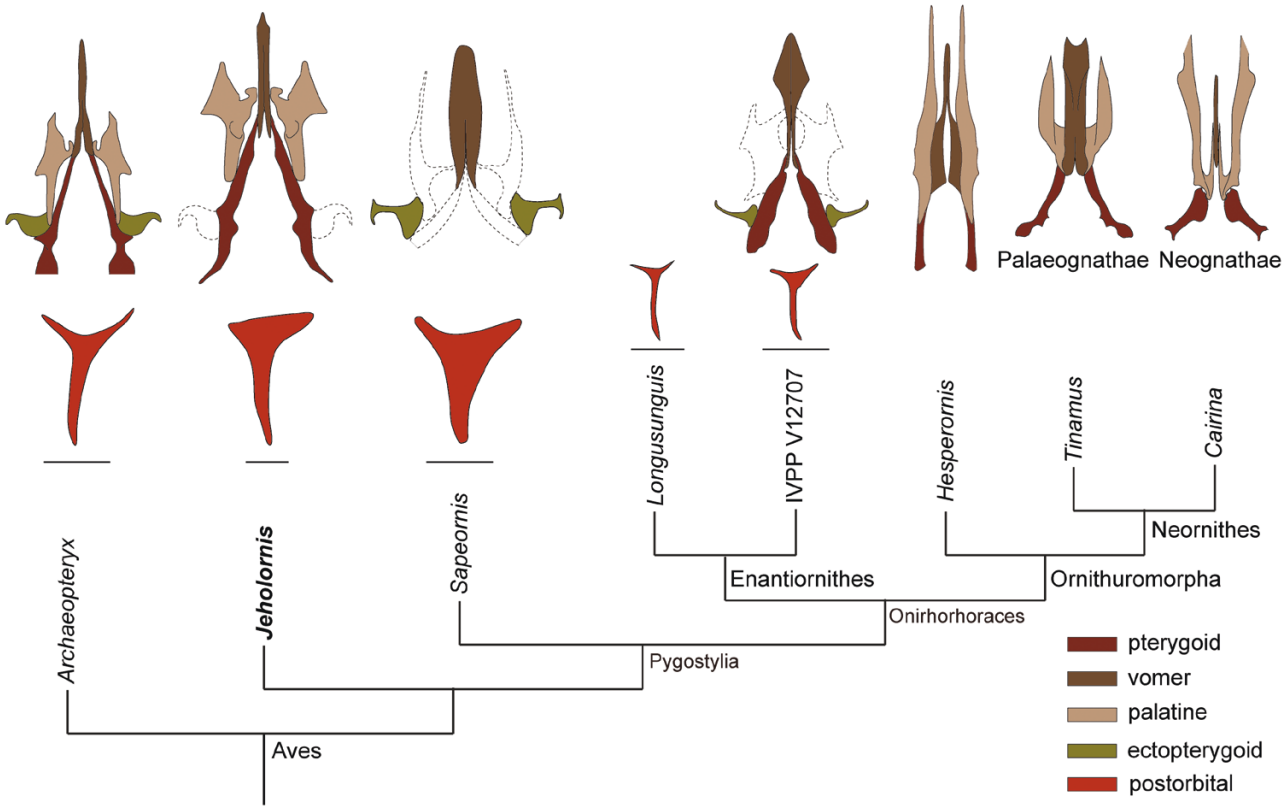

Figure 6. Comparisons of postorbital and palatal complex in Aves. Taxa without the postorbital present indicate that this element has been entirely reduced and fused to the frontal to be the postorbital process in these taxa. Dashed lines indicate uncertain structures. Scale bar: 5 mm only for the postorbitals.

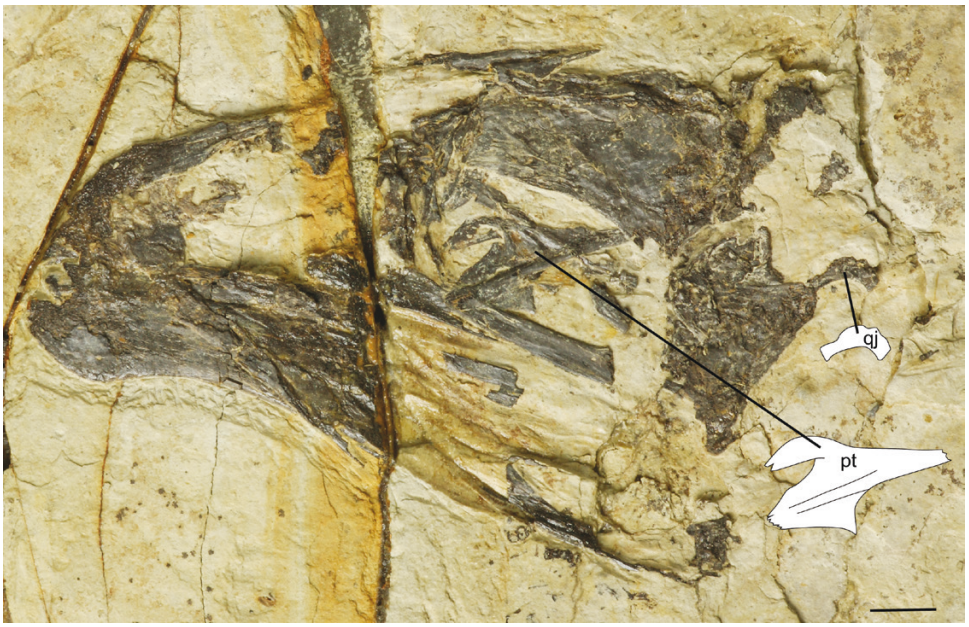

Figure 7. Photograph and reidentified cranial elements of *Jeholornis palmapenis*. Scale bar: 5 mm. Revised from O'Connor *et al.* (2012). Abbreviations: pt, palatine; qj, quadratojugal.

2022). The palatine ramus is slender and might contact the parasphenoid rostrum and/or the pterygoid ramus of vomer rostrally. The quadrate ramus of the pterygoid is well developed and extrudes dorsally from the main body, indicating a large, lateromedial contact with the quadrate. The presence of a basipterygoid process like that present in *Archaeopteryx* and enantiornithine IVPP V12707 cannot be determined owing to mediolateral crushing in STM 3-8 (Elżanowski & Wellnhofer, 1996; Wang *et al.*, 2021).

Scleral ring

Specimen STM 3-8 preserves both scleral rings (Fig. 5G, H), although some scleral ossicles might have been lost during preservation. Each individual ossicle is nearly rectangular, with subequal margins. The articular facet for the adjacent ossicle forms approximately one-quarter of the surface, except for overplates (scleral ossicles that overlap both adjacent ossicles). The 3D models of the best-preserved and the most *in situ* articulated plates were used to reconstruct the complete scleral ring, suggesting that it consisted of a total of 15 ossicles.

Dentary

Both mandibles are completely preserved, with the right one slightly disarticulated, in STM 3-8 (Fig. 8). The dentaries are not fused at the symphysis and curve rostroventrally along their entire length (Fig. 8C, D). Nevertheless, the dorsal margin of the dentary is only weakly convex. The symphysis is expanded ventrally such that the rostral one-third of the ventral margin of the dentary is more strongly convex, giving a rostrally downturned appearance. The rostral margin of the symphysis is inclined caudoventrally. The lateral surface of the dentary is marked by several neurovascular foramina rostrally. The alveolar shelf is well developed along the dorsomedial margin.

The caudal margin of the dentary of *Jeholornis* is forked, as in *Sapeornis* but with a much longer ventral ramus, whereas the dorsal ramus is longer in *Sapeornis* (Hu *et al.*, 2020a). However, the weakly forked condition in both *Sapeornis* and *Jeholornis*, in which one process is much shorter than the other, contrasts with the strongly forked condition in confuciusornithiforms and neornithines (Chiappe *et al.*, 1999; Elżanowski *et al.*, 2018; Wang *et al.*, 2019a) and the unforked condition reported in most enantiornithines (O'Connor & Chiappe, 2011). The caudal half of the dentary is excavated laterally by a large, concave fossa. Meckel's groove, which is located on the medial surface of dentary, is either shallow or absent, whereas it is well developed in *Archaeopteryx* and non-avialan theropods (Elżanowski & Wellnhofer, 1996; Rauhut, 2003; Norman *et al.*, 2004). Meckel's groove is also present in *Ichthyornis* and some enantiornithines (O'Connor *et al.*, 2013b; Field *et al.*, 2018; Wang *et al.*, 2021), although comparisons are limited by the paucity of medially preserved dentaries among Mesozoic birds.

Three alveoli are located rostrally in the dentary and house small teeth, with crown heights ~80% that of maxillary teeth. The dentary teeth are different from the maxillary teeth, being smaller in size and less expanded at the root, strongly resembling the dentary teeth of *Sapeornis*, which are interpreted as having reduced functionality (Wang *et al.*, 2017a; Hu *et al.*, 2020a). The alveoli are separated by interdental bone, resulting in interdental spaces of similar lengths to the tooth diameters. Another similar-sized tooth is dislocated and preserved close to both the right maxilla and the right dentary (Fig. 8F). This tooth is additional to the count pertaining to the combined maxillae and dentaries (ten alveoli in total, but 11 teeth are present) and might represent a disarticulated replacement tooth, consistent with the absence of a root. Despite being more similar to the size of the maxillary teeth, owing to the incomplete preservation of the roots of both maxillary and dentary teeth, it cannot be determined confidently which tooth is the functional tooth related to this replacement tooth. The rostral-most portion of the dentary, rostral to the first dentary tooth, is excavated by a shallow concavity; a similar structure was also reported in some Mesozoic ornithuromorphs (Dumont *et al.*, 2016; O'Connor *et al.*, 2022).

Postdentary bones

The prearticular and the articular are entirely fused to the surangular (Fig. 8G–I). The surangular is shorter than the dentary and has a well-developed dorsally projecting coronoid process on its caudal half. Cranial to the coronoid process the surangular tapers rostrally, articulating with the lateral surface of the dentary. In medial view, a shallow mandibular fossa excavates the surangular above the prearticular. A narrow rostral mandibular fenestra is visible, defined ventrally by the prearticular and dorsally by the surangular, and a caudal mandibular fenestra is absent, whereas in *Confuciusornis* both the rostral and caudal mandibular fenestrae are well developed (Chiappe *et al.*, 1999; Elżanowski *et al.*, 2018; Wang *et al.*, 2019a).

The angular is small and positioned underneath the surangular and dentary (Fig. 8L, M). The articular lacks the dorsal deflection present in *Sapeornis*, more resembling that of *Archaeopteryx* (Hu *et al.*, 2020a). No pneumatic foramen is present in the articular. The medial cotyle is broader than the lateral cotyle, divided by the intercotylar crest. The medial process is not tapered. The retroarticular process is weakly developed.

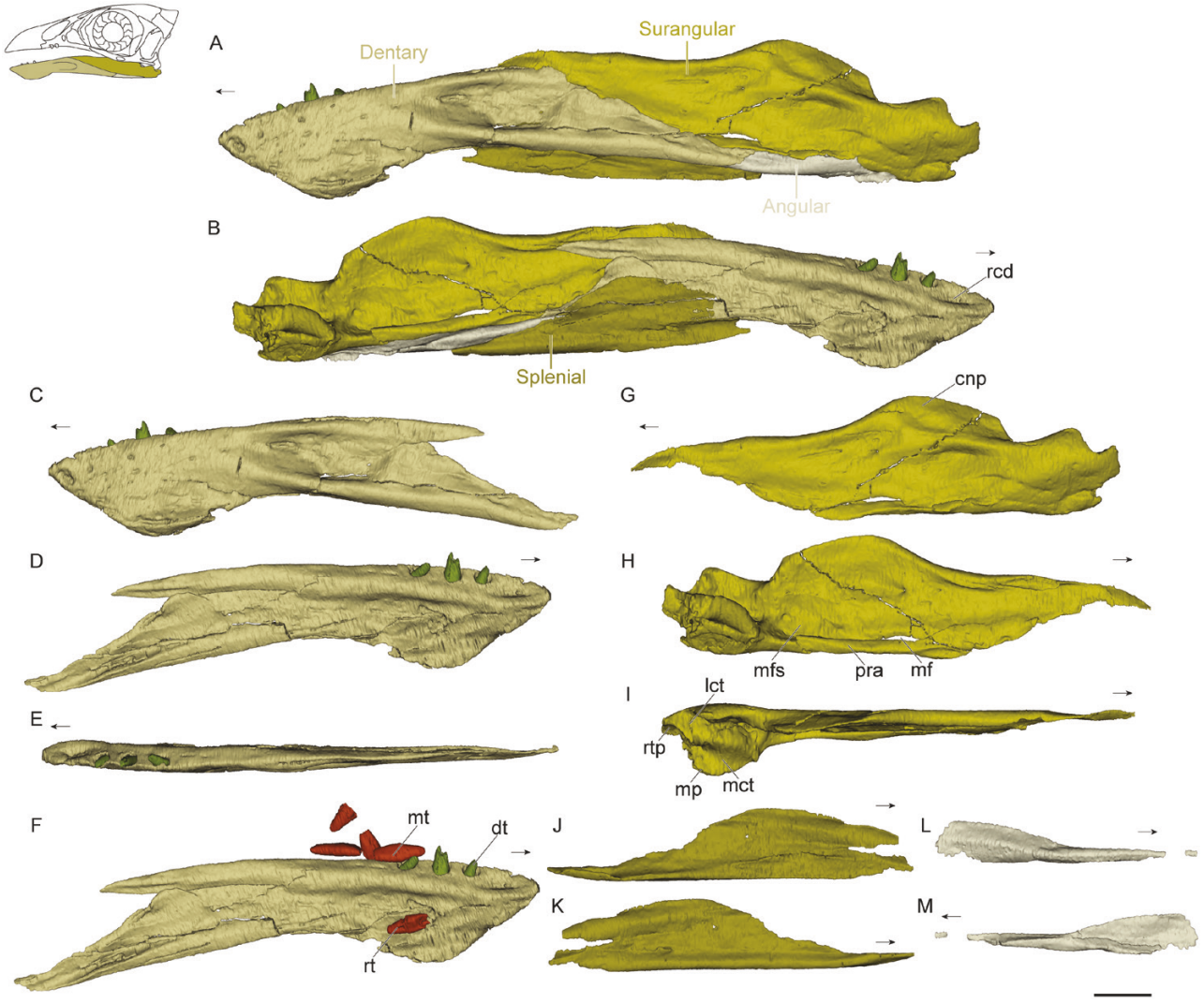

Figure 8. Three-dimensional snapshots of mandibular elements of *Jeholornis* STM 3-8: lateral (A) and medial (B) views of the left mandible; lateral (C), medial (D) and dorsal (E) views of the left dentary; medial view of the left dentary with maxillary teeth (F); lateral (G), medial (H) and dorsal (I) views of the left surangular; lateral (J) and medial (K) views of the right splenial; lateral (L) and medial (M) views of the angular. Scale bar: 5 mm. Arrows indicate the rostral direction. Abbreviations: cnp, coronoid process; dt, dentary teeth; lct, lateral condyle; mct, medial condyle; mf, mandibular fenestra; mfs, mandibular fossa; mp, medial process; mt, maxillary teeth; pra, prearticular; rcd, rostral concavity of dentary; rt, replacement tooth; rtp, retroarticular process.

The splenial is triangular in lateral profile (Fig. 8J, K). The rostral wing is short and ends abruptly; the caudal wing is long, slender and sharply tapered, and the dorsal wing is broadly convex, defining an obtuse angle.

DENTITION

To determine the accurate dentition of *Jeholornis* and whether the presence or absence of maxillary teeth is diagnostic among species (O'Connor *et al.*, 2012), 83 jeholornithiform specimens were examined based on the STM and IVPP collections (main slab and counter slab are counted as one specimen). All specimens were preliminarily referred to *Jeholornis*, based on their large body size, long bony tail, sternum with lateral trabecula absent and expanded caudalmost pair of sternal ribs (Zheng *et al.*, 2014). Of these 83 specimens, teeth are preserved in 24 specimens (Supporting Information, Table S2), among which the presence and number of dentary teeth could be evaluated by either dentary teeth *in situ* or clearly observable alveoli in the dentary in 17 specimens. Of these 17 specimens, three dentary teeth are preserved

in four specimens (STM 2-3 counter slab, 2-38, 2-49 and 3-8), and no more than three dentary teeth are preserved in any specimen (Supporting Information, Table S2). Identified by their proportionately small size, disarticulated dentary teeth were identified in three specimens (STM 2-40, 3-5 counter slab and 3-6). Only four specimens exhibit a laterally exposed and unbroken dentary with no visible dentary teeth (STM 2-15, 2-46, 3-13 and 3-16). However, the presence of teeth cannot be ruled out, because the alveolar margin is not exposed and disarticulated teeth in other specimens indicate that teeth can fall free of their alveoli post-mortem. No specimen preserves unequivocal evidence of the absence of dentary teeth.

In situ maxillary teeth or clearly observable alveoli in the maxilla are preserved in 14 specimens. Among them, two maxillary teeth are preserved in eight specimens (STM 2-3 counter slab, 2-4, 2-30, 2-37, 2-50, 2-54, 3-8 and 3-32), and no more than two maxillary teeth are preserved in any specimen. One maxillary tooth is visible in another six specimens (STM 2-2 main and counter slabs, 2-7, 2-14, 2-45, 2-55 and 3-33 counter slab). Most of these teeth represent a single, similar morphology and are larger than the dentary teeth. However, in STM 2-45, 2-55 and 3-33 counter slab, the single visible maxillary tooth is remarkably smaller than those in other specimens, indicating that they are in the early stages of erupting. Displaced maxillary teeth are also identified based on their relatively large size in another four specimens (STM 2-2 main and counter slabs, 2-13, 2-40 and 2-49). Four specimens exhibit an unbroken, intact ventral margin of the maxilla and an absence of maxillary teeth (STM 2-15, 2-24, 2-38 and 2-39).

Maxillary teeth are not preserved in STM 2-37, but two empty alveoli are clearly visible, and the teeth of the right maxilla of STM 2-37, which is buried in the matrix, are also displaced, with two empty alveoli. Combined with the presence of the displaced maxillary/dentary teeth in other specimens, this could suggest that the maxillary/dentary teeth of the jeholornithiforms easily fall out of the alveoli and are lost during the preservation process, resulting in an artificial variance in the dentition number across individuals. Although the ventral margins of the maxilla and the dorsal margins of the dentary are intact but lacking teeth or alveoli in a few specimens, it should be noted that if the teeth were displaced and the alveoli filled by the matrix, it would be difficult to observe the alveoli in those 2D slabs that lack professional preparation.

Together, these observations strongly suggest that the dentition in all jeholornithiforms is 0–2–3 (number of premaxillary teeth–number of maxillary teeth–number of dentary teeth).

Emended diagnosis of *J. prima*

Based on the morphological study of this specimen, we provide the following revised diagnosis for *J. prima*. A large stem bird with the following combination of features: premaxilla edentulous with short maxillary process; two teeth with blunt crowns in maxilla and three relatively smaller teeth in dentary (new); paired, sheet-like preorbital ossifications present near the nasals (new, autapomorphy); C-shaped lacrimal with short rostrodorsal ramus and lacrimal foramen (new); unreduced postorbital forming a complete postorbital bar with jugal (new); pterygoid rami of vomer much longer than the fused rostral portion, expanded in the middle and lacking the caudodorsal process (new); palatine with broad pterygoid wing and jugal process (new); narrow and restricted mandibular fenestra between prearticular and surangular (new); 27 caudal vertebrae in total, with the transition point occurring after the fifth vertebra; lateral trabecula of sternum absent; caudalmost pair of sternal ribs expanded; first phalanx of the third manual digit twice as long as the second phalanx; ratio of forelimb (humerus plus ulna plus carpometacarpus) to hindlimb (femur plus tibiotarsus plus tarsometatarsus) of ~1.2:1; dorsal margin of the ilium nearly straight and craniodorsal–caudoventrally oriented (modified from Zhou & Zhang, 2002; O'Connor *et al.*, 2012; Zheng *et al.*, 2020).

Biology of *Jeholornis*

The olfactory bulb-to-forebrain ratio suggests that olfaction was important in *Jeholornis*, indicated by a higher value in comparison to closely related stem birds, such as *Archaeopteryx* and *Confuciusornis* (Supporting Information, Table S3). The proportions seen in *Jeholornis* are more similar to more basal coelurosaurs, such as *Bambiraptor* Burnham *et al.*, 2000, *Garudimimus* Barsbold, 1981 (an ornithomimosaur) and *Dilong* Xu *et al.*, 2004 (an early-diverging tyrannosauroid) (Zelenitsky *et al.*, 2011).

To test quantitatively another important sensory ability (vision) of *Jeholornis*, we measured the orbital length and the scleral ring outer/inner diameters of STM 3-8, using the protocol described by Choiniere *et al.* (2021; Fig. 9). With the addition of these data, we reran 'Analysis 5' in the phylogenetic flexible discriminant analysis of the scleral ring and orbit morphology described by Choiniere *et al.* (2021), because their analysis has the most accurate posterior classification rates among all other versions of similar analyses (Choiniere *et al.*, 2021). The results indicate an inference of diurnal habits in *Jeholornis* (posterior probability of being nocturnal < 0.01; Supporting Information, Table S4).

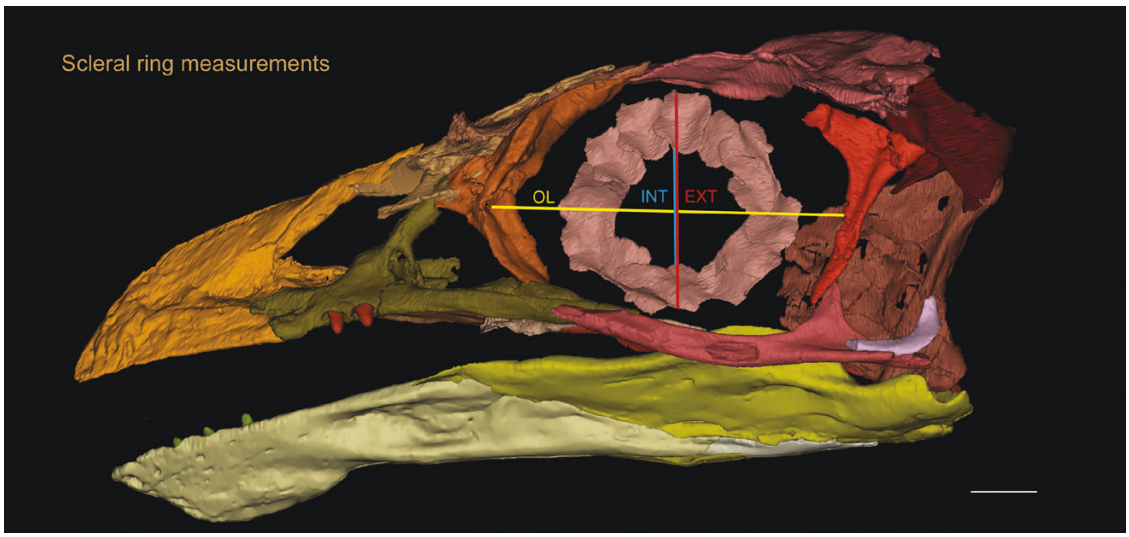

Figure 9. Scleral ring measurements of *Jeholornis* STM 3-8. Reassembled three-dimensional cranial model of *Jeholornis* STM 3-8 used for measurements, following Hu *et al.* (2022). Scale bar: 5 mm. Abbreviations: EXT, scleral ring outer diameter; INT, scleral ring inner diameter; OL, orbital length.

DISCUSSION

Only four stem avian skulls have previously been described in detail based on high-resolution computed tomography or synchrotron scanning data: *Archaeopteryx* (Kundrát *et al.*, 2018), enantiornithine IVPP V12707 (Wang *et al.*, 2021), *Falcatakely* O'Connor *et al.*, 2020 (O'Connor *et al.*, 2020) and the ornithuromorph *Ichthyornis* (Field *et al.*, 2018). With the addition of the new data from *Jeholornis*, these five taxa sample the entire Mesozoic phylogeny of birds, making it possible to begin to elucidate patterns in avian cranial evolution. The information provided by them reveal the unique evolutionary pathways taken by each lineage, especially the differences in palatal morphology and brain shape. These detailed studies also help to clarify controversial or poorly understood aspects of the cranial morphology of these taxa, such as the dentition, and some palaeobiological aspects of *Jeholornis*.

The dentition and potential variation of the dentition of *Jeholornis* have previously been unclear. Among most previously published specimens of *Jeholornis*, the dentition is described as having zero to three dentary teeth and lacking teeth in the upper jaw (Supporting Information, Table S1; Ji *et al.*, 2002b; Zhou & Zhang, 2002, 2003; Lefèvre *et al.*, 2014; Wang *et al.*, 2020a) or ambiguously, with 'a few small, blunt teeth on the back of the upper jaw' (Chiappe & Meng, 2016). Therefore, the presence of maxillary teeth was used as one of the diagnostic features of a new species of *Jeholornis*, *J. palmapenis* (O'Connor *et al.*, 2012). The 3D scans of *Jeholornis* STM 3-8 allow assessment of the number of alveoli present, revealing that the dental formula in this individual is 0–2–3, which is confirmed to be the complete dentition of *Jeholornis* based on our observation of a large sample size of this lineage.

The presence of maxillary dentition is thus not considered to be diagnostic of *J. palmapenis*. Other purported interspecific differences currently used to support different species of jeholornithiforms are also subtle (Zhou & Zhang, 2002; O'Connor *et al.*, 2012; Lefèvre *et al.*, 2014; Wang *et al.*, 2020a). However, a detailed investigation of the taxonomy of the Jeholornithiformes is beyond the scope of the present study of cranial anatomy.

The observed variation in body size in the 83 specimens investigated here has tentatively been interpreted as indicative of different ontogenetic stages. However, this is not yet supported by osteohistological evidence, and interspecific variation in size, as observed in other paravians (Chiappe *et al.*, 1999), cannot be ruled out at this time.

The relatively 3D preservation of the cranial elements in *Jeholornis* STM 3-8 also reveals the first information regarding the brain of *Jeholornis*, filling an important gap between *Archaeopteryx* and the Ornithuromorpha (Alonso *et al.*, 2004; Fabbri *et al.*, 2017). Overall, the brain morphology appears more similar to *Archaeopteryx* (Alonso *et al.*, 2004; Balanoff *et al.*, 2013; Fabbri *et al.*, 2017; Beyrand *et al.*, 2019) than to crown birds.

The size of the olfactory bulbs is a proxy for olfactory capabilities in vertebrates (Edinger & Rand, 1908; Jerison, 1973; Corfield *et al.*, 2015), and the relative size of the olfactory bulbs in comparison to the forebrain is widely used to infer olfaction capabilities

in non-avian dinosaurs, birds and other vertebrates (Healy & Guilford, 1990; Clark *et al.*, 1993; Steiger *et al.*, 2008, 2009; Zelenitsky *et al.*, 2011; Corfield *et al.*, 2015). Given that no significant correlation between body mass and the relative olfactory bulb size in Aves (including stem and crown) was found in previous studies (Zelenitsky *et al.*, 2011), olfactory capabilities can be inferred reliably even in Mesozoic stem birds, in which the typically crushed, 2D preservation of limb elements makes body mass inferences problematic. Our comparisons of the olfactory bulb ratio between stem and crown Paraves and *Jeholornis* indicate that olfaction might be important to *Jeholornis*, and enhanced olfactory capabilities might have played a role in feeding, navigation, individual recognition or reproduction.

Besides olfaction, visual function can also be inferred from the morphology of the orbit and scleral ring and used to determine the diel activity pattern of fossil vertebrates, including dinosaurs and early birds (Schmitz & Motani, 2011; Choiniere *et al.*, 2021). The digital reconstruction of the scleral ring of *Jeholornis* STM 3-8 shows a relatively narrow aperture compared with the orbit diameter (Fig. 9), suggesting diurnal habits. Our quantitative analysis of the visual ability of *Jeholornis* based on the scleral rings confirms this hypothesis that it possessed diurnal habits, similar to other Mesozoic birds investigated so far (*Archaeopteryx*, *Confuciusornis*, *Sapeornis* and *Yixianornis* Zhou & Zhang, 2001; Schmitz & Motani, 2011; Choiniere *et al.*, 2021; Supporting Information, Table S4).

This information increases our understanding of the life habits of this key taxon during the origin and early evolutionary stage of birds, supporting inferences that diurnal activity patterns dominated in early-diverging avian lineages (Aves) (Schmitz & Motani, 2011; Choiniere *et al.*, 2021). The likelihood of widespread diurnal habits in Early Mesozoic birds is consistent with the high frequency of diurnal habits seen in extant birds (Martin, 2010) but differs from the more balanced occurrence of both nocturnality and diurnality in non-avian theropods, including strong evidence for specialized nocturnality in some groups (Schmitz & Motani, 2011; Choiniere *et al.*, 2021). This raises the possibility that a transition to diel activity patterns more similar to those of modern birds occurred around the origins of Aves or shortly afterwards.

ACKNOWLEDGEMENTS

This research is part of a project that has received funding from the European Union's Horizon 2020 research and innovation programme under the Marie Skłodowska-Curie grant agreement number 101024572. It is also supported by project ZR2020MD026, Shandong Provincial Natural Science Foundation, China; Linyi Key Research and Development Project 2020ZX028; and the National Natural Science Foundation of China grants 42288201, 41402017 and 42002016. H.H., Y.W., P.G.M., S.W., Z.Z. and R.B.J.B. designed the research; H.H., Y.W., J.K.O., X.Y., X.Z. and R.B.J.B. wrote the anatomical descriptions; M.F. carried out the neurocranial anatomical analyses; H.H. and R.B.J.B carried out the scleral ring analyses; and H.H., M.F, J.K.O. and R.B.J.B. wrote the paper. We are grateful to the editors and two reviewers for their constructive comments, which improved the manuscript. The authors declare no competing interests.

DATA AVAILABILITY

The key specimen for this project, *Jeholornis* STM 3-8, is housed and available for future researchers to check at the Shandong Tianyu Museum of Nature, China. The original computed tomography scanning slices and segmented STL files of *Jeholornis* STM 3-8 are available in MorphoSource (https://www.morphosource.org/projects/0000C1212).

REFERENCES

Alonso PD, **Milner AC**, **Ketcham RA**, **Cookson MJ**, **Rowe TB. 2004**. The avian nature of the brain and inner ear of *Archaeopteryx*. *Nature* **430**: 666–669.

Balanoff AM, **Bever GS**, **Rowe TB**, **Norell MA. 2013**. Evolutionary origins of the avian brain. *Nature* **501**: 93–96.

Barsbold R, **Osmólska H. 1999**. The skull of *Velociraptor* [Theropoda] from the Late Cretaceous of Mongolia. *Acta Palaeontologica Polonica* **44**: 189–219.

Baumel JJ, **Witmer LM. 1993**. Osteologia. In: Baumel JJ, King AS, Breazile JE, Evans HE, Vanden Berge JC, eds. *Handbook of avian anatomy: nomina anatomica avium*, 2nd edn. Cambridge: Nuttall Ornithological Club, 45–132.

Beyrand V, **Voeten DFAE**, **Bureš S**, **Fernandez V**, **Janáček J**, **Jirák D**, **Rauhut O**, **Tafforeau P. 2019**. Multiphase progenetic development shaped the brain of flying archosaurs. *Scientific Reports* **9**: 10807.

Chiappe LM, **Ji SA**, **Ji Q**, **Norell MA. 1999**. Anatomy and systematics of the Confuciusornithidae (Theropoda, Aves) from the late Mesozoic of northeastern China. *Bulletin of the American Museum of Natural History* **242**: 1–89.

Chiappe LM, **Meng Q. 2016**. *Birds of stone: Chinese avian fossils from the age of dinosaurs*. Baltimore: Johns Hopkins University Press.

Chiappe LM, **Norell M**, **Clark J. 2001**. A new skull of *Gobipteryx minuta* (Aves: Enantiornithes) from the Cretaceous of the Gobi Desert. *American Museum Novitates* **3346**: 1–15.

Choiniere JN, **Neenan JM**, **Schmitz L**, **Ford DP**, **Chapelle KEJ**, **Balanoff AM**, **Sipla JS**, **Georgi JA**, **Walsh SA**, **Norell MA**, **Xu X**, **Clark JM**, **Benson RBJ. 2021**. Evolution of vision and hearing modalities in theropod dinosaurs. *Science* **372**: 610–613.

Clark JM, **Norell MA**, **Rowe T. 2002**. Cranial anatomy of *Citipati osmolskae* (Theropoda, Oviraptorosauria), and a reinterpretation of the holotype of *Oviraptor philoceratops*. *American Museum Novitates* **2002**: 1–24.

Clark L, **Avilova KV**, **Bean NJ. 1993**. Odor thresholds in passerines. *Comparative Biochemistry and Physiology Part A: Physiology* **104**: 305–312.

Corfield JR, **Price K**, **Iwaniuk AN**, **Gutierrez-Ibañez C**, **Birkhead T**, **Wylie DR. 2015**. Diversity in olfactory bulb size in birds reflects allometry, ecology, and phylogeny. *Frontiers in Neuroanatomy* **9**: 102.

Dumont M, **Tafforeau P**, **Bertin T**, **Bhullar BA**, **Field D**, **Schulp A**, **Strilisky B**, **Thivichon-Prince B**, **Viriot L**, **Louchart A. 2016**. Synchrotron imaging of dentition provides insights into the biology of *Hesperornis* and *Ichthyornis*, the 'last' toothed birds. *BMC Evolutionary Biology* **16**: 178.

Edinger L, **Rand HW. 1908**. The relations of comparative anatomy to comparative psychology. *Journal of Comparative Neurology and Psychology* **18**: 437–457.

Elżanowski A. 1991. New observations of the skull of *Hesperornis* with reconstructions of the bony palate and otic region. *Postilla* **207**: 1–20.

Elżanowski A, **Peters DS**, **Mayr G. 2018**. Cranial morphology of the Early Cretaceous bird *Confuciusornis*. *Journal of Vertebrate Paleontology* **38**: e1439832.

Elżanowski A, **Stidham TA. 2010**. Morphology of the quadrate in the Eocene anseriform *Presbyornis* and extant galloanserine birds. *Journal of Morphology* **271**: 305–323.

Elżanowski A, **Wellnhofer P. 1996**. Cranial morphology of *Archaeopteryx*: evidence from the seventh skeleton. *Journal of Vertebrate Paleontology* **16**: 81–94.

Fabbri M, **Koch NM**, **Pritchard AC**, **Hanson M**, **Hoffman E**, **Bever GS**, **Balanoff AM**, **Morris ZS**, **Field DJ**, **Camacho J**, **Rowe TB**, **Norell MA**, **Smith RM**, **Abzhanov A**, **Bhullar BAS. 2017**. The skull roof tracks the brain during the evolution and development of reptiles including birds. *Nature Ecology & Evolution* **1**: 1543–1550.

Field DJ, **Benito J**, **Chen A**, **Jagt JWM**, **Ksepka DT. 2020**. Late Cretaceous neornithine from Europe illuminates the origins of crown birds. *Nature* **579**: 397–401.

Field DJ, **Hanson M**, **Burnham D**, **Wilson LE**, **Super K**, **Ehret D**, **Ebersole JA**, **Bhullar BAS. 2018**. Complete *Ichthyornis* skull illuminates mosaic assembly of the avian head. *Nature* **557**: 96–100.

Gao C, **Liu J. 2005**. A new avian taxon from Lower Cretaceous Jiufotang Formation of western Liaoning. *Global Geology* **24**: 313–318.

He HY, **Wang XL**, **Zhou ZH**, **Wang F**, **Boven A**, **Shi GH**, **Zhu RX. 2004**. Timing of the Jiufotang Formation (Jehol Group) in Liaoning, northeastern China, and its implications. *Geophysical Research Letters* **31**: L12605.

Healy S, **Guilford T. 1990**. Olfactory-bulb size and nocturnality in birds. *Evolution* **44**: 339–346.

Hu H, **O'Connor JK**, **McDonald PG**, **Wroe S. 2020a**. Cranial osteology of the Early Cretaceous *Sapeornis chaoyangensis* (Aves: Pygostylia). *Cretaceous Research* **113**: 104496.

Hu H, **O'Connor JK**, **Wang M**, **Wroe S**, **McDonald PG. 2020b**. New anatomical information on the bohaiornithid *Longusunguis* and the presence of a plesiomorphic diapsid skull in Enantiornithes. *Journal of Systematic Palaeontology* **18**: 1481–1495.

Hu H, **Sansalone G**, **Wroe S**, **McDonald PG**, **O'Connor JK**, **Li Z**, **Xu X**, **Zhou Z. 2019**. Evolution of the vomer and its implications for cranial kinesis in Paraves. *Proceedings of the National Academy of Sciences of the United States of America* **116**: 19571–19578.

Hu H, **Wang Y**, **McDonald PG**, **Wroe S**, **O'Connor JK**, **Bjarnason A**, **Bevitt JJ**, **Yin X**, **Zheng X**, **Zhou Z**, **Benson RBJ. 2022**. Earliest evidence for fruit consumption and potential seed dispersal by birds. *eLife* **11**: e74751.

Jerison HJ. 1973. *Evolution of the brain and intelligence*. New York and London: Academic Press, 340–362.

Ji Q, **Ji S**, **You H**, **Zhang J**, **Yuan C**, **Ji X**, **Li J**, **Li Y**, **Downs TBW. 2002a**. Discovery of an Avialae bird from China, *Shenzhouraptor sinensis* gen. et sp. nov. *Geological Bulletin of China* **21**: 363–369.

Ji Q, **Ji S**, **Zhang H**, **You H**, **Zhang J**, **Wang L**, **Yuan C**, **Ji X. 2002b**. A new avialian bird *Jixiangornis orientalis* gen. et sp. nov. from the Lower Cretaceous of western Liaoning, NE China. *Journal of Nanjing University (Natural Sciences)* **38**: 723–736.

Kundrát M, **Nudds J**, **Kear BP**, **Lü J**, **Ahlberg P. 2018**. The first specimen of *Archaeopteryx* from the Upper Jurassic Mörnsheim Formation of Germany. *Historical Biology* **31**: 3–63.

Lefèvre U, **Hu D**, **Escuillié F**, **Dyke G**, **Godefroit P. 2014**. A new long-tailed basal bird from the Lower Cretaceous of north-eastern China. *Biological Journal of the Linnean Society* **113**: 790–804.

Martin G. 2010. *Birds by night*. London: A&C Black.

Mayr G, **Pohl B**, **Hartman S**, **Peters DS. 2007**. The tenth skeletal specimen of *Archaeopteryx*. *Zoological Journal of the Linnean Society* **149**: 97–116.

Norman DB, **Sues HD**, **Witmer LM**, **Coria RA. 2004**. *The Dinosauria*. Berkeley: University of California Press, 393–412.

O'Connor JK, **Chiappe LM. 2011**. A revision of enantiornithine (Aves: Ornithothoraces) skull morphology. *Journal of Systematic Palaeontology* **9**: 135–157.

O'Connor JK, **Chiappe LM**, **Gao C**, **Zhao B. 2011**. Anatomy of the Early Cretaceous enantiornithine bird *Rapaxavis pani*. *Acta Palaeontologica Polonica* **56**: 463–475.

O'Connor JK, **Stidham TA**, **Harris JD**, **Lamanna MC**, **Bailleul AM**, **Hu H**, **Wang M**, **You H. 2022**. Avian skulls represent a diverse ornithuromorph fauna from the Lower Cretaceous Xiagou Formation, Gansu Province, China. *Journal of Systematics and Evolution* **60**: 1172–1198.

O'Connor JK, **Sun C**, **Xu X**, **Wang X**, **Zhou Z. 2012**. A new species of *Jeholornis* with complete caudal integument. *Historical Biology* **24**: 29–41.

O'Connor JK, **Wang M**, **Hu H. 2016**. A new ornithuromorph (Aves) with an elongate rostrum from the Jehol Biota, and

the early evolution of rostralization in birds. *Journal of Systematic Palaeontology* **14**: 939–948.

O'Connor JK, **Wang X**, **Sullivan C**, **Wang Y**, **Zheng X**, **Hu H**, **Zhang X**, **Zhou Z. 2018**. First report of gastroliths in the Early Cretaceous basal bird *Jeholornis*. *Cretaceous Research* **84**: 200–208.

O'Connor JK, **Wang X**, **Sullivan C**, **Zheng X**, **Tubaro P**, **Zhang X**, **Zhou Z. 2013a**. Unique caudal plumage of *Jeholornis* and complex tail evolution in early birds. *Proceedings of the National Academy of Sciences of the United States of America* **110**: 17404–17408.

O'Connor JK, **Zhang Y**, **Chiappe LM**, **Meng Q**, **Quanguo L**, **Di L. 2013b**. A new enantiornithine from the Yixian formation with the first recognized avian enamel specialization. *Journal of Vertebrate Paleontology* **33**: 1–12.

O'Connor JK, **Zheng XT**, **Hu H**, **Wang XL**, **Zhou ZH. 2017**. The morphology of *Chiappeavis magnapremaxillo* (Pengornithidae: Enantiornithes) and a comparison of aerodynamic function in Early Cretaceous avian tail fans. *Vertebrata Palasiatica* **55**: 41–58.

Rauhut OW. 2003. *Special papers in palaeontology, the interrelationships and evolution of basal theropod dinosaurs*. London: Blackwell Publishing.

Rauhut OWM. 2014. New observations on the skull of *Archaeopteryx*. *Paläontologische Zeitschrift* **88**: 211–221.

Rauhut OWM, **Foth C**, **Tischlinger H. 2018**. The oldest *Archaeopteryx* (Theropoda: Avialiae): a new specimen from the Kimmeridgian/Tithonian boundary of Schamhaupten, Bavaria. *PeerJ* **6**: e4191.

Sanz JL, **Chiappe LM**, **Pérez-Moreno BP**, **Moratalla JJ**, **Hernández-Carrasquilla F**, **Buscalioni AD**, **Ortega F**, **Poyato-Ariza FJ**, **Rasskin-Gutman D**, **Martínez-Delclòs X. 1997**. A nestling bird from the Lower Cretaceous of Spain: implications for avian skull and neck evolution. *Science* **276**: 1543–1546.

Schmitz L, **Motani R. 2011**. Nocturnality in dinosaurs inferred from scleral ring and orbit morphology. *Science* **332**: 705–708.

Smith-Paredes D, **Núñez-León D**, **Soto-Acuña S**, **O'Connor J**, **Botelho JF**, **Vargas AO. 2018**. Dinosaur ossification centres in embryonic birds uncover developmental evolution of the skull. *Nature Ecology & Evolution* **2**: 1966–1973.

Steiger SS, **Fidler AE**, **Kempenaers B. 2009**. Evidence for increased olfactory receptor gene repertoire size in two nocturnal bird species with well-developed olfactory ability. *BMC Evolutionary Biology* **9**: 117.

Steiger SS, **Fidler AE**, **Valcu M**, **Kempenaers B. 2008**. Avian olfactory receptor gene repertoires: evidence for a well-developed sense of smell in birds? *Proceedings of the Royal Society B: Biological Sciences* **275**: 2309–2317.

Tsuihiji T, **Barsbold R**, **Watabe M**, **Tsogtbaatar K**, **Chinzorig T**, **Fujiyama Y**, **Suzuki S. 2014**. An exquisitely preserved troodontid theropod with new information on the palatal structure from the Upper Cretaceous of Mongolia. *Naturwissenschaften* **101**: 131–142.

Wang M, **Hu H. 2017**. A comparative morphological study of the jugal and quadratojugal in early birds and their dinosaurian relatives. *The Anatomical Record* **300**: 62–75.

Wang M, **Hu H**, **Li Z. 2015**. A new small enantiornithine bird from the Jehol Biota, with implications for early evolution of avian skull morphology. *Journal of Systematic Palaeontology* **14**: 481–497.

Wang M, **Jingmai K**, **Zhou Z. 2019a**. A taxonomical revision of the Confuciusornithiformes (Aves: Pygostylia). *Vertebrata Palasiatica* **57**: 1–37.

Wang M, **Li Z**, **Liu Q**, **Zhou Z. 2020b**. Two new Early Cretaceous ornithuromorph birds provide insights into the taxonomy and divergence of Yanornithidae (Aves: Ornithothoraces). *Journal of Systematic Palaeontology* **18**: 1805–1827.

Wang M, **O'Connor JK**, **Pan Y**, **Zhou Z. 2017b**. A bizarre Early Cretaceous enantiornithine bird with unique crural feathers and an ornithuromorph plough-shaped pygostyle. *Nature Communications* **8**: 14141.

Wang M, **O'Connor JK**, **Zhou S**, **Zhou Z. 2019b**. New toothed Early Cretaceous ornithuromorph bird reveals intraclade diversity in pattern of tooth loss. *Journal of Systematic Palaeontology* **18**: 631–645.

Wang M, **Stidham TA**, **Li Z**, **Xu X**, **Zhou Z. 2021**. Cretaceous bird with dinosaur skull sheds light on avian cranial evolution. *Nature Communications* **12**: 3890.

Wang M, **Zhou Z. 2018**. A new confuciusornithid (Aves: Pygostylia) from the Early Cretaceous increases the morphological disparity of the Confuciusornithidae. *Zoological Journal of the Linnean Society* **185**: 417–430.

Wang X, **Huang J**, **Kundrát M**, **Cau A**, **Liu X**, **Wang Y**, **Ju S. 2020a**. A new jeholornithiform exhibits the earliest appearance of the fused sternum and pelvis in the evolution of avialan dinosaurs. *Journal of Asian Earth Sciences* **199**: 104401.

Wang Y, **Hu H**, **O'Connor JK**, **Wang M**, **Xu X**, **Zhou Z**, **Wang X**, **Zheng X. 2017a**. A previously undescribed specimen reveals new information on the dentition of *Sapeornis chaoyangensis*. *Cretaceous Research* **74**: 1–10.

Watanabe A, **Gignac PM**, **Balanoff AM**, **Green TL**, **Kley NJ**, **Norell MA. 2019**. Are endocasts good proxies for brain size and shape in archosaurs throughout ontogeny? *Journal of Anatomy* **234**: 291–305.

Witmer LM. 1997. The evolution of the antorbital cavity of archosaurs: a study in soft-tissue reconstruction in the fossil record with an analysis of the function of pneumaticity. *Journal of Vertebrate Paleontology* **17**: 1–76.

Xu L, **Buffetaut E**, **O'Connor J**, **Zhang X**, **Jia S**, **Zhang J**, **Chang H**, **Tong H. 2021**. A new, remarkably preserved, enantiornithine bird from the Upper Cretaceous Qiupa Formation of Henan (central China) and convergent evolution between enantiornithines and modern birds. *Geological Magazine* **158**: 2087–2094.

Xu X, **Pittman M**, **Sullivan C**, **Choiniere JN**, **Tan Q**, **Clark JM**, **Norell MA**, **Wang S. 2015**. The taxonomic status of the Late Cretaceous dromaeosaurid *Linheraptor exquisitus* and its implications for dromaeosaurid systematics. *Vertebrata Palasiatica* **53**: 29–62.

Xu X, **Wu XC. 2001**. Cranial morphology of *Sinornithosaurus millenii* Xu *et al*. 1999 (Dinosauria: Theropoda: Dromaeosauridae) from the Yixian Formation of Liaoning, China. *Canadian Journal of Earth Sciences* **38**: 1739–1752.

Xu X, **Zhou Z**, **Wang Y**, **Wang M. 2020**. Study on the Jehol Biota: recent advances and future prospects. *Science China Earth Sciences* **63**: 757–773.

Yin YL, **Pei R**, **Zhou CF. 2018**. Cranial morphology of *Sinovenator changii* (Theropoda: Troodontidae) on the new material from the Yixian Formation of western Liaoning, China. *PeerJ* **6**: e4977.

Zelenitsky DK, **Therrien F**, **Ridgely RC**, **McGee AR**, **Witmer LM. 2011**. Evolution of olfaction in non-avian theropod dinosaurs and birds. *Proceedings of the Royal Society B: Biological Sciences* **278**: 3625–3634.

Zhang Z, **Chiappe LM**, **Han G**, **Chinsamy A. 2013**. A large bird from the Early Cretaceous of China: new information on the skull of enantiornithines. *Journal of Vertebrate Paleontology* **33**: 1176–1189.

Zheng X, **O'Connor J**, **Wang X**, **Wang M**, **Zhang X**, **Zhou Z. 2014**. On the absence of sternal elements in *Anchiornis* (Paraves) and *Sapeornis* (Aves) and the complex early evolution of the avian sternum. *Proceedings of the National Academy of Sciences of the United States of America* **111**: 13900–13905.

Zheng X, **Sullivan C**, **O'Connor JK**, **Wang X**, **Wang Y**, **Zhang X**, **Zhou Z. 2020**. Structure and possible ventilatory function of unusual, expanded sternal ribs in the Early Cretaceous bird *Jeholornis*. *Cretaceous Research* **116**: 104597.

Zhou Z. 2014. The Jehol Biota, an Early Cretaceous terrestrial Lagerstätte: new discoveries and implications. *National Science Review* **1**: 543–559.

Zhou Z, **Clarke J**, **Zhang F. 2008**. Insight into diversity, body size and morphological evolution from the largest Early Cretaceous enantiornithine bird. *Journal of Anatomy* **212**: 565–577.

Zhou Z, **Wang Y. 2010**. Vertebrate diversity of the Jehol Biota as compared with other lagerstätten. *Science China Earth Sciences* **53**: 1894–1907.

Zhou Z, **Zhang F. 2002**. A long-tailed, seed-eating bird from the Early Cretaceous of China. *Nature* **418**: 405–409.

Zhou Z, **Zhang F. 2003**. *Jeholornis* compared to *Archaeopteryx*, with a new understanding of the earliest avian evolution. *Naturwissenschaften* **90**: 220–225.

Zhou Z, **Zhang F. 2007**. Mesozoic birds of China—a synoptic review. *Frontiers of Biology in China* **2**: 1–14.

SUPPORTING INFORMATION

Additional Supporting Information may be found in the online version of this article at the publisher's web-site:

Table S1. List of the published jeholornithids with cranial elements described.
Table S2. List of *Jeholornis* specimens preserving teeth *in situ* examined in this study.
Table S3. Comparisons of the olfactory bulb ratio between stem and crown Paraves and *Jeholornis* (following Zelenitsky *et al.*, 2011, except for *Jeholornis*).
Table S4. Posterior probability of nocturnality for extinct avemetatarsalians in the phylogenetic flexible discriminant analysis by Choiniere *et al.* (2021), with *Jeholornis* added into the dataset.